

1 **Supplementary Information**

2

3 **A multi-dimensional, time-lapse, high content screening**

4 **platform applied to schistosomiasis drug discovery**

5

6 **Steven Chen¹, Brian M Suzuki^{2,3}, Jakob Dohrmann⁴, Rahul Singh^{4*}, Michelle R**

7 **Arkin^{1*} & Conor R Caffrey^{2,3*}**

8 ¹Department of Pharmaceutical Chemistry and Small Molecule Discovery Center,

9 University of California, San Francisco, CA 94143; ²Center for Discovery and Innovation

10 in Parasitic Diseases, Department of Pathology, University of California, San Francisco,

11 CA 94158; ³Center for Discovery and Innovation in Parasitic Diseases, Skaggs School

12 of Pharmacy and Pharmaceutical Sciences, University of California, San Diego, La Jolla,

13 CA 92093; ⁴Department of Computer Science, San Francisco State University, San

14 Francisco, CA 94132

15

16 *correspondence to: rahul@sfsu.edu; michelle.arkin@ucsf.edu;

17 ccaffrey@health.ucsd.edu.

18

19	Contents	
20	Supplementary Table 1	page 3
21	Supplementary Figure 1	page 5
22	Supplementary Figure 2	page 7
23	Supplementary Figure 3	page 8
24	Supplementary Figure 4	page 9
25	Supplementary Figure 5	page 10
26	Supplementary Figure 6	page 11
27	Extended Methods	page 12
28		

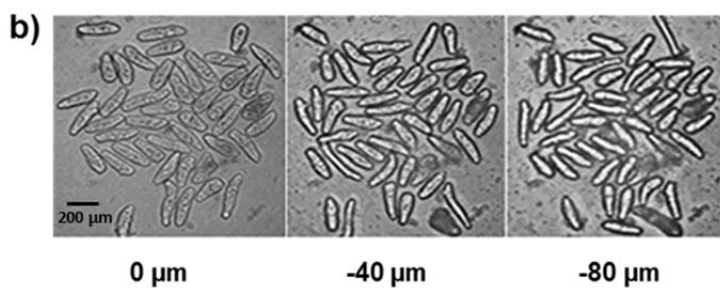
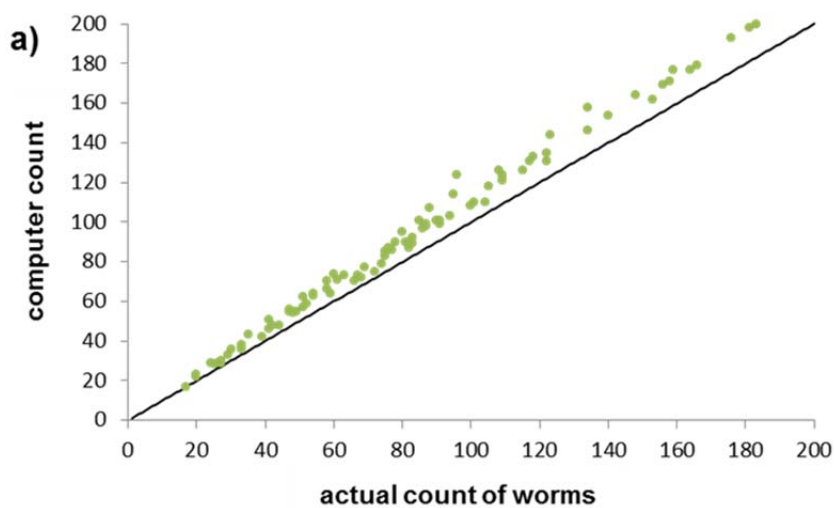
29 **Supplementary Table 1.** Glossary of Terms.

Term	Description	Units
Area	Area of a target	μm^2
Median Diameter	The median internal distance perpendicular to the maximum curved chord.	μm
Length	Maximum distance across a target. Boundaries may be crossed.	μm
Form Factor	Estimate of circularity, expressed as a value between 0 and 1 (1 equals a perfect circle).	value
Perimeter	Distance around a target.	μm
Straight Chord	The maximum straight-line distance across a target without crossing a boundary.	μm
Curved Chord	Maximum center line through target.	μm
Bend	Bend = (max curved chord / max straight chord).	ratio
Pinch	Pinch = (median diameter * length) / area) is the estimated area divided by the actual area.	ratio
Wave	Wave = Perimeter / (2 * Area ^{0.5}) is the actual perimeter divided by the estimated perimeter.	ratio
Mass	The sum of all pixel values in the shape.	sum
WMOI	(Weighted Moment of Inertia) Index of the homogeneity of density levels (gray levels) within a circular target. A value of 1 indicates the target is relatively homogeneous. If >1, the target has a higher proportion of bright pixels in its center. If <1, the target has a higher proportion of bright pixels around its perimeter.	index
Density levels	Gray level intensity, where black = 0 and white = 4095 (12-bit image).	Levels
SD - Levels	A standard deviation (SD) of pixel densities, which measures the pixel density variation within the target.	levels
Angle	Angle of the straight chord relative to the horizontal (horizontal = 0 degrees). Negative values are clockwise from horizontal; positive values are counter-clockwise.	degrees

Rate	The average amount of changes between sequential time-lapse images.	"units"/frame
Frequency	The number of times a feature changes direction.	Hz
Effect Size (ES)	ES = $(x-\mu)/\sigma$ where x is the drug mean, μ is the DMSO mean, and σ is the standard deviation of DMSO. No unit, but the magnitude of the measurement can be thought of as the number of standard deviations from the DMSO control group for the selected feature.	
Mahalanobis Distance (d_M)	d_M is a multi-dimensional effect size which measures the distance of a test point from a reference distribution. No unit, but the magnitude of the measurement can be thought of as the number of standard deviations from the DMSO control group.	

30

31



32

c)

Time (h)	Precision	Recall	DMSO/DRUG treated worms used
2	0.93	0.97	19,567
24	0.86	0.97	19,643
48	0.88	0.89	19,246
Time Range (h)	Precision	Recall	Total Worms
2 - 48	0.88	0.95	58,456 (40.6 worms/well over 1440 wells)

33

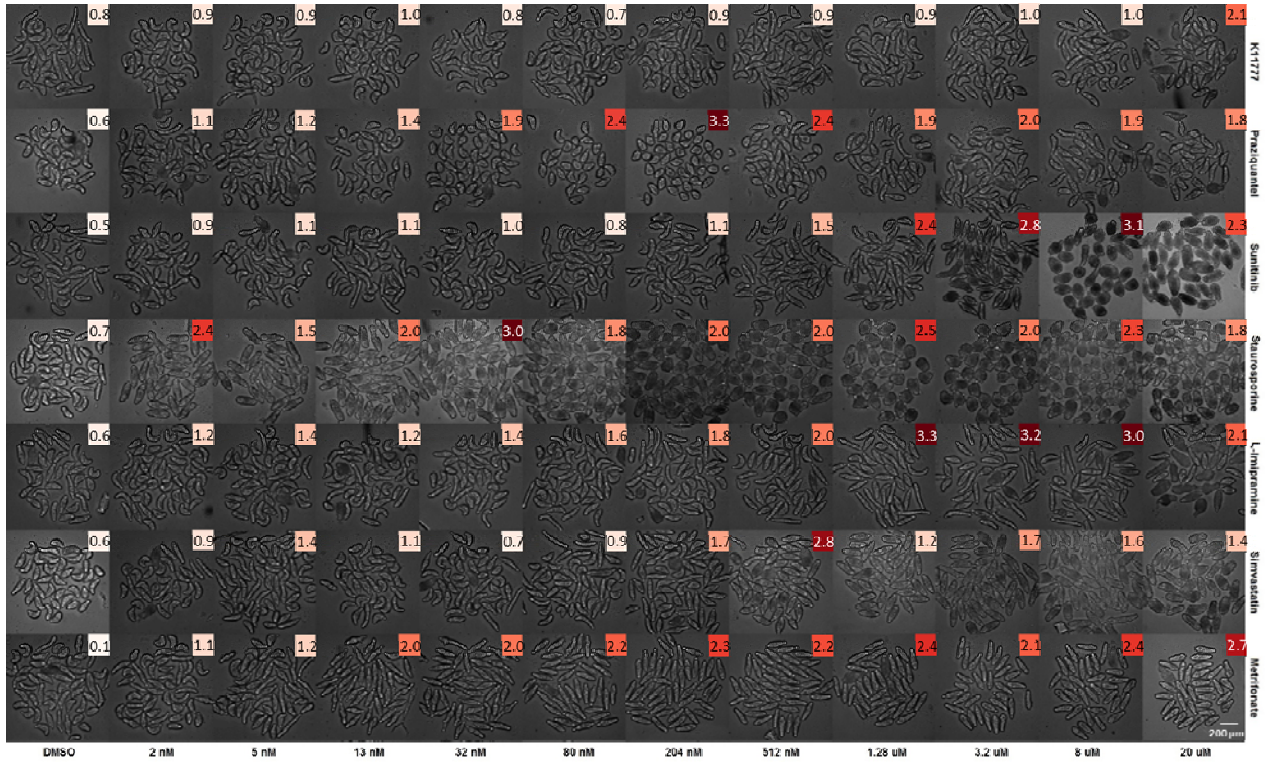
d)

Time (h)	%DMSO Treated Worms Overlapped	%DMSO Treated Worms Not Analyzed Due To Overlap	DMSO Treated Worms Used in Overlap Analysis
2	0.053	0	3,764
24	0.053	0.053	3,754
48	0.47	0.31	3,598

34

35

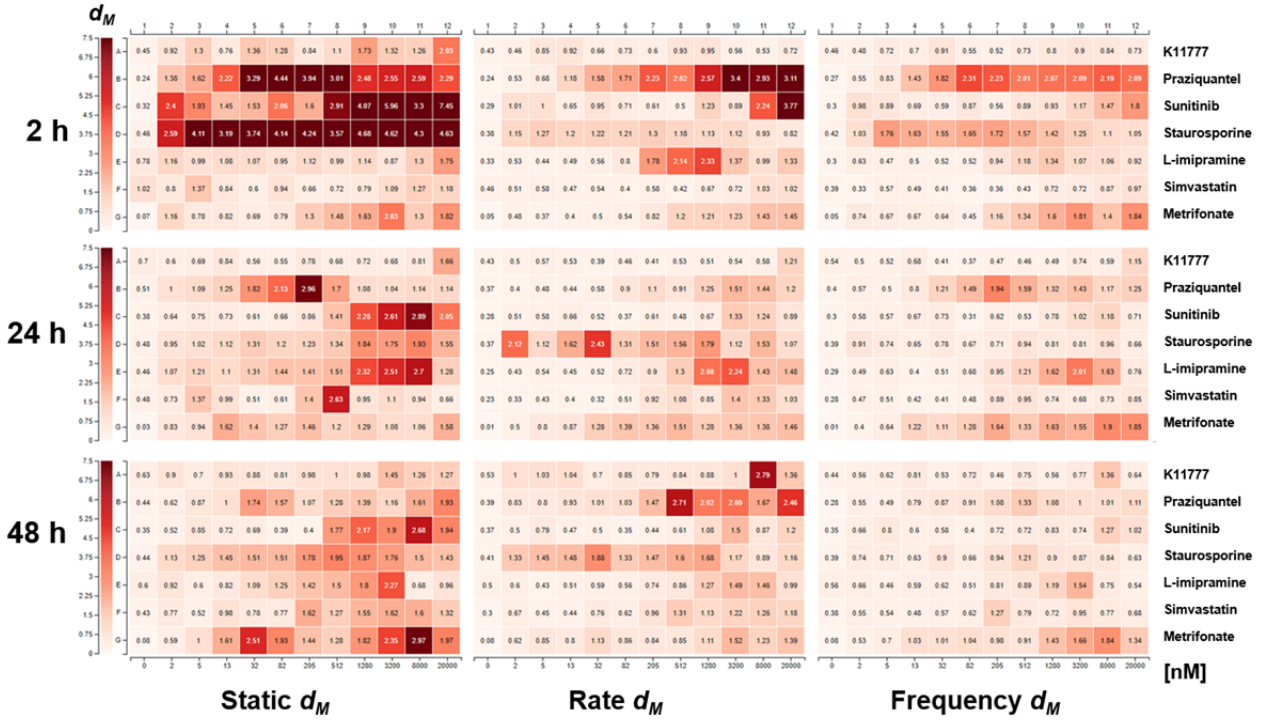
36 **Supplementary Figure 1.** Optimizing parasite handling and segmentation. **(a)** Comparison of actual
37 somules (counted by visual inspection) and the number of somules identified by the object classifier
38 algorithm 'computer count' (see **Extended Methods**, below). Computational inclusion of non-worm
39 objects with worm-like features leads to a systematic 10% increase in object count. **(b)** Images from a
40 single sample well imaged at three focal planes (0, -40, and -80 μm from the outside bottom of the
41 well). Lowering the focal plane improves the contrast of the somule outline ('edge'); at -40 μm the
42 appearance of the outline is improved while some of the internal texture detail is preserved. **(c)**
43 Precision and recall were determined by manual inspection of the 58,456 somules that were screened
44 in the seven-drug set. **(d)** Somule overlap frequency and data removal due to overlap events. The
45 overlap increases from 0.05% to 0.3-0.47% between 24 and 48 h, potentially reflecting growth of the
46 somules, increased degeneracy or increased motility.
47



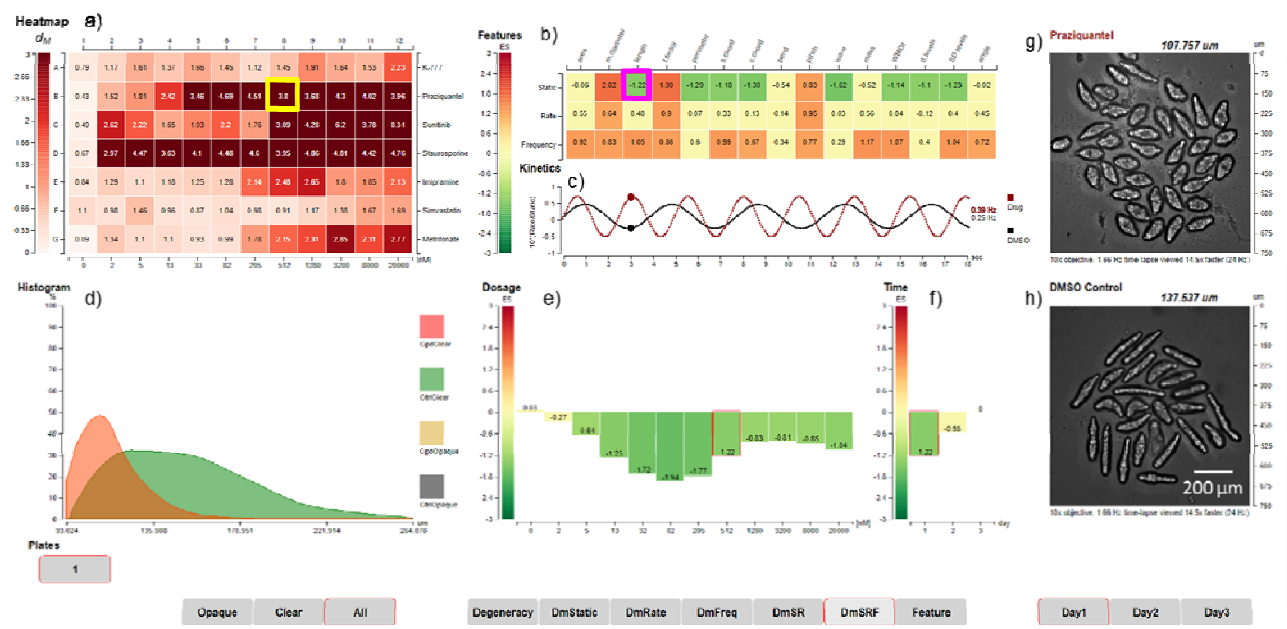
48
49

50 **Supplementary Figure 2.** Montage of somule images 24 h after treatment with seven test drugs. Drug
51 names are to the right and concentrations are at the bottom. Each image in the montage is labeled with
52 the corresponding d_M value and scaled color.

53
54
55

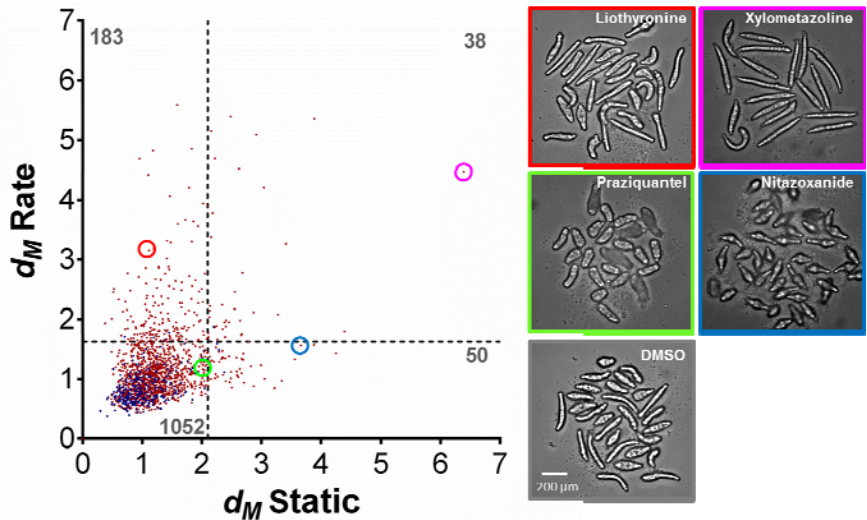


Supplementary Figure 3. Differing sensitivities of d_M measurements in the static, rate and frequency modes. d_M values at 2, 24 or 48 h after treatment were measured using only static features (left panels), rate (center panels) or frequency for seven test drugs. Drugs were arrayed over an 11-point 2.5-fold dilution range from 2 nM to 20 μ M. Values were determined from the aggregation of four wells per treatment. Note that the d_M values shown do not necessarily smoothly change with increasing dose of drug. This complexity reflects the observation that multiple parameters show maximum changes at different concentrations. Each mode offers a differential sensitivity to measuring changes in the somule; e.g., the static d_M for staurosporine across all concentrations after 2 h, the rate d_M for imipramine (205 – 1280 nM) after 2 h and the frequency d_M for metrifonate at 8 and 20 μ M after 24 h.



71
72
73
74
75
76
77
78
79
80
81
82
83
84
85
86
87
88
89
90
91
92
93
94
95
96
97

Supplementary Figure 4. Screenshot of the SchistoView graphical user interface. The figure is analogous to **Fig 3**, but highlights the length of PZQ-treated somules whereas **Fig 3** shows the frequency of changes in length. Selected data are shown to illustrate the hierarchical approach to visualization. **(a)** Heat map of Mahalanobis distances (d_M) for seven test drugs arrayed over an 11-point 2.5-fold dilution series from 2 nM in column 2 to 20 μ M in column 12. Drugs, from top to bottom, are, K11777, PZQ, sunitinib, staurosporine, imipramine, simvastatin and metrifonate. DMSO controls are arrayed in column 1 and are shown as the average d_M (0.77) for all DMSO controls. A d_M of 1.61 is significantly different (3 SD) from control. Clicking on coordinate B8 (identified by the yellow square: 512 nM PZQ) populates panels **(b)** and **(g)** (see below). **(b)** Heat map showing the effect sizes (ES) for static, rate and frequency, after exposure to 512 nM PZQ for 2 h, *i.e.*, the selected well from **(a)**. Three sets of 15 features are arrayed in rows and columns, respectively. Clicking on the intersection of the length feature and static mode (magenta box) in **(b)** populates panels **(c)** through **(f)** and the underlying data. **(c)** Calculated waveforms defined by the range of length (amplitude) and frequency of length contraction (frequency). DMSO control worms are slower moving (lower frequency) than those treated with 512 nM PZQ (red line). **(d)** Histogram displaying the distribution of static length for DMSO control worms (green) and PZQ-treated worms (orange). **(e)** Bar graph depicting the ES for static length after PZQ treatment across 11 concentrations (second row in **(a)**). **(f)** Bar graph depicting the ES for static length in the 512 nM PZQ treatment across the three days of measurement. **(g)** First image from time-lapsed movie of the well highlighted in **(a)**; in the live SchistoView, the 30-frame movie is looped. **(h)** as for **(g)** except for the DMSO control.



98

99

100

101

102

103

104

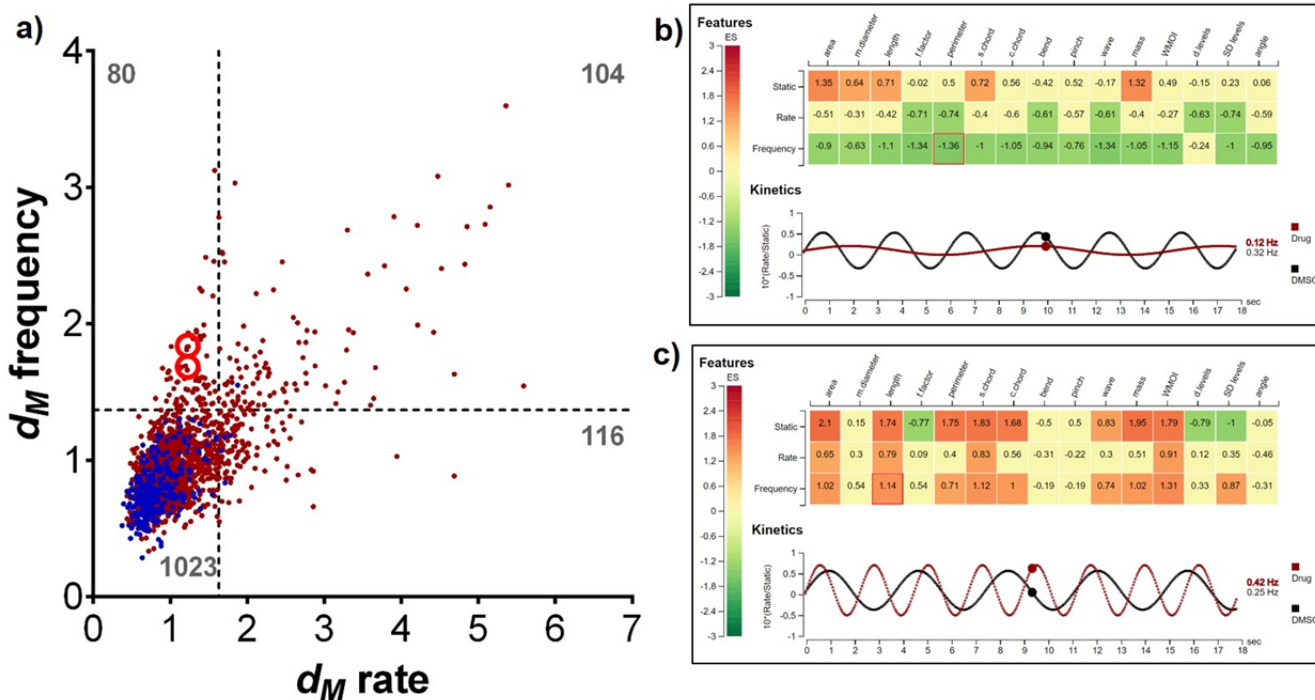
105

106

107

108

Supplementary Figure 5. Scatterplot of $d_{M(rate)}$ vs. $d_{M(static)}$ for a primary screen of 1,323 approved drugs. Like **Fig 6b** in the main text, which shows a scatterplot of $d_{M(frequency)}$ vs. $d_{M(static)}$, the screen was performed at 10 μ M. The data shown are from the first scan cycle approximately 24 h after the addition of drug. The dashed lines represent the d_M values that are 3 SD from the DMSO mean (2.1 for $d_{M(static)}$ and 1.6 for $d_{M(rate)}$). The number of drugs in each quadrant is indicated in dark grey for both static and rate modes: 1,052 drugs were inactive, 50 drugs induced static phenotypes only, 183 induced only kinetic phenotypes and 38 compounds induced changes in both modes. The frames of the images to the right are color-matched with the highlighted compounds in the plot: note the remarkable range of phenotypes presented by this parasite.



109

110 **Supplementary Figure 6.** (a) Scatterplot of d_M (frequency) vs. d_M (rate) for a primary screen of 1,323 approved
 111 drugs. Like Fig. 6b in the main text which shows a scatterplot of d_M (frequency) vs. d_M (static), the screen was
 112 performed at 10 μ M. The data shown are from the first scan cycle approximately 24 h after the addition
 113 of drug. The dashed lines represent the d_M values that are 3 SD from the DMSO mean (1.6 for d_M for rate and 1.4 for d_M for frequency). The number of drugs in each quadrant is indicated in dark grey for
 114 both frequency and rate modes: 1,023 drugs were inactive, 116 drugs induced significant rate-based
 115 phenotypes only, 80 induced phenotypes associated with frequency only and 104 compounds induced
 116 changes in both modes. Two drugs, vilazodone and apomorphine, are marked with upper and lower red
 117 circles, respectively. (b, c) Examples of drugs that induce more changes in frequencies than changes in
 118 rates as shown by the table of Features (effect sizes) and Kinetics (red = drug; black = DMSO).
 119 Apomorphine (b) induces a hypomotile phenotype, whereas vilazodone (c) generates hypermotility.
 120 Images taken from SchistoView.
 121

122

123

125 **Time-lapse Image Acquisition**

126 Open the automation scheduler (Momentum 2.0) with instructions to move each assay plate from
127 the automated tissue culture incubator (Thermofisher C2, 37°C, 5% CO₂) to the barcode reader, then to
128 the automated microscope (GE IN Cell Analyzer 2000), and then back to the tissue culture incubator.
129 One cycle takes approximately 35 minutes or the time it takes to scan one assay plate in the automated
130 microscope.

131

132 1. Place the 96-well round bottom polystyrene assay plate with lid (Costar 3799) into the nest of a
133 GE IN Cell Analyzer 2000 (software version 3.0.0.43).

134 2. Open the acquisition protocol with the following settings (from XDCE):

135

a. Objective

136

i. Focal length = 20.0

137

ii. Id = 12111

138

iii. Lineartype = 7

139

iv. Magnification = 10

140

v. Numerical Aperture = 0.45

141

vi. Objective Name = 10X/0.45, Plan Apo, CFI/60

142

vii. Pixel height = 2.96

143

viii. Pixel width = 2.96

144

ix. Refractive index = 1.0

145

x. Unit = μm

146

b. Polychroic

147

i. QUAD1 (any polychroic will do)

148

c. CCD Camera

149

i. Size; height = 2048, width = 2048

150

ii. Flat Field Correction = False

151

iii. Binning value = 4 x 4

152

iv. Bias value = 144.21

153

v. Gain value = ""

154

d. Wavelength

155

i. Imaging mode = 2-D

156

ii. Excitation Filter = TL-Brightfield, 473 nM

157

iii. Emission Filter = DAPI, 455 nM

158

iv. Exposure time = 3 ms

159

v. HWAFOffset = 0 μm

160

vi. FocusOffset = -50 μm

161

e. Software Auto Focus = False

162

f. Laser Auto Focus = True

163

g. Plate dimensions as entered in software

164

i. Columns = 12, Rows = 8

165

ii. Plate height = 14.16 mm

166

iii. Bottom thickness = 1310 μm

- 167 iv. Bottom interface = plastic
- 168 v. Bottom height = 2.15 mm
- 169 vi. Well volume = 360 uL
- 170 vii. Well parameters = Round, Size = 6.35 mm
- 171 viii. Top Left Well Center Offset ; horizontal = 13.8 mm, vertical = 11.7 mm
- 172 ix. Well Spacing; horizontal = 9.0 mm, vertical = 9.0 mm
- 173 h. Plate heater use = false
- 174 i. Plate map, acquisition mode
 - 175 i. Layout; columns = 1, rows = 1
 - 176 ii. Direction value = horizontal snake
- 177 j. Time schedule = enabled
 - 178 i. Incubate between time points = false
 - 179 ii. Mode = spit and stare
 - 180 iii. Time points in ms = 0, 3740, 4340, 4940, 5540, 6140, 6740, 7340, 7940, 8540,
 - 181 9140, 9740, 10340, 10940, 11540, 12140, 12740, 13340, 13940, 14540, 15140,
 - 182 15740, 16340, 16940, 17540, 18140, 18740, 19340, 19940, 20540, 21140
 - 183 1. This first time point = 0 is the point at which the autofocus operation
 - 184 occurs. To allow time for this operation to complete, the next time point
 - 185 occurs at 3740 ms and continues at a rate of 600 ms between time lapse
 - 186 images. In total, there were 1 autofocus image and 30 time lapse images.
- 187 3. Write the image stack to an E-SATA connected storage device (preferably RAID) capable of
- 188 storing 1.44 GB per assay plate per day.

189 The exposure time of 3 ms (step 2.d.iv) is the shortest exposure time the GE IN Cell Analyzer 2000
 190 will accept. With the CCD camera binning value set to 4 x 4 (step 2.c.iii), some of the pixels in the
 191 image may be saturated (>= 4095). The binning value of 4 x 4 allowed for the fastest time lapse
 192 acquisition of 600 milliseconds since a smaller array is faster to readout. The possibility of saturated
 193 pixels was accepted in return for a faster frame rate.

194 **Image Segmentation** (*Protocol: Schisto94*)

195 Open IN Cell Developer Toolbox 1.9 which can be found in IN Cell Investigator 1.6, a suite of
 196 software that comes with the GE IN Cell Analyzer 2000 automated microscope. From the “analysis” tab,
 197 select “batch analysis manager...” and “add...”, select the “Schisto94_ba” protocol, and image folders
 198 for analysis. Then select “Run batch analysis...”

199 There are three main workflows: clear body outliner, tegument outliner, dark body outliner.
 200 These workflows are imaging preprocessing macros which transform the image prior to segmentation.
 201 Each workflow produces 4 target types: threshold 1, threshold 2, threshold 3, and a merge of the
 202 results from threshold 1 to 3. Each target set records 17 features: area, x, y, diameter, length, form
 203 factor, perimeter, straight chord, curved chord, bend (a user defined feature), pinch (a user defined
 204 feature), wave (a user defined feature), mass, weighted moment of inertia, density-levels, sd-levels,
 205 and angle. The data is recorded at the cell level, or in this case, per organism.

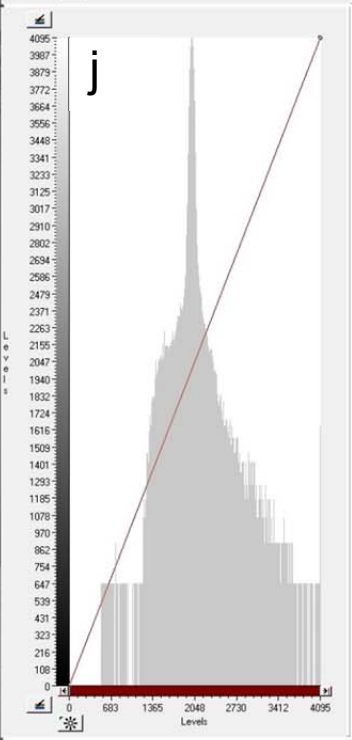
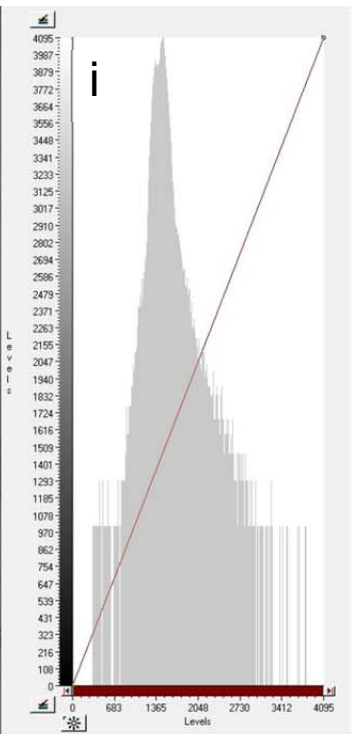
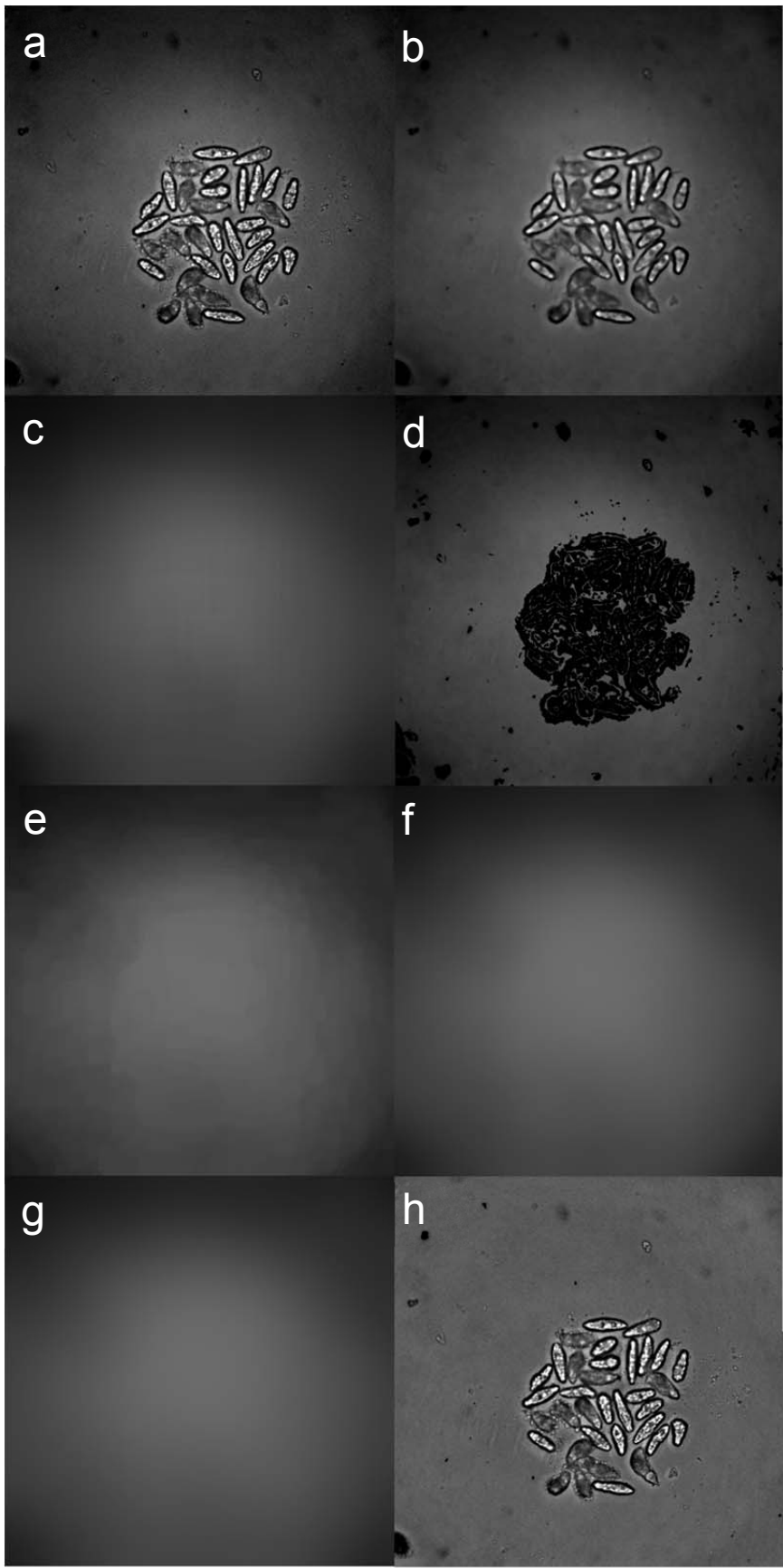
206 The purpose of this segmentation is to cast a large net around a large variety of objects where
 207 up to 50% could be artefactual (i.e. inter-organism objects, intra-organism objects). This inefficiency is

208 by design in order to lower the false negative rate in segmentation. The false positives (artifacts) are
209 detected and removed in a subsequent data processing step external to IN Cell Developer 1.9

210 Before any of the workflows are run, the raw image is processed with a custom built flat field
211 correction (FFC) image preprocessing macro. All subsequent processing and analysis will be based on
212 the flat field corrected image. (The flat field correction is the first step in the Macro:
213 *schisto94_n_master*.)

- 214 1. **Flat Field Correction** (Macro: *Schisto94_a_FFC*) (**Figure 1**). Divide the raw image by an
215 estimate of the background of each image to produce a flat field correction. The steps below
216 outline how an estimate was generated. (Code enumerated in roman numerals) (8 operations
217 per image)
 - 218 a. Load raw image.
 - 219 b. Transform result from step “1.a” with transform filter = median, kernel size = 5
 - 220 c. Transform result from step “1.b” with transform filter = local arithmetic
 - 221 i. kernel = 99;
 - 222 ii. src = IAve;
 - 223 d. Apply a transform point operation = arithmetic (two src) where source1 = result from step
224 “1.b” and source2 = result from step “1.c”.
 - 225 i. $\text{Sel}(\text{abs}(\text{src1}-\text{src2})/\text{src2}<0.025,\text{src1},0)$;
 - 226 e. Transform result from step “1.d” with transform filter = max, kernel size = 33
 - 227 f. Transform result from step “1.e” with transform filter = local arithmetic
 - 228 i. kernel = 51;
 - 229 ii. src = IAve;
 - 230 g. Transform result from step “1.f” with transform filter = local arithmetic
 - 231 i. kernel = 67;
 - 232 ii. src = IAve;
 - 233 h. Apply a transform point operation = arithmetic (two src) where source1 = result from step
234 “1.a” and source2 = result from step “1.g”.
 - 235 i. $(\text{src1}/\text{src2})*2048$;

236 The round wells of the 96-well assay plate produce varying backgrounds due to the position of
237 the well in the plate, the artefacts in the plastic, and changes in illumination due to the grayness of the
238 sample. Therefore, an *in situ* background estimate was used. Flat field correction and centering of the
239 pixel values in each image allows for the universal application of object detection thresholds based on
240 fixed values.



242 **Figure 1, Flat Field Correction using an *in situ* background estimate.** a) raw image, b) median
243 transform of raw image (light smoothing), c) local arithmetic transform of raw image (heavy smoothing),
244 d) transform point operation which sets pixel in panel "b" to zero if pixel is > 2.5% different from the
245 same pixel in panel "c", e) max transform promotes background pixels between and around zeroed
246 pixels in panel "d", f) local arithmetic transform smooths result from panel "e", g) local arithmetic
247 transform smooths result from panel "f", h) transform point operation which divides the raw image by
248 the background estimate in panel "g" and then multiplies the result by 2048 to center the image pixel
249 values within the 12-bit range, i) histogram of the raw image, j) histogram of the flat field corrected
250 image.

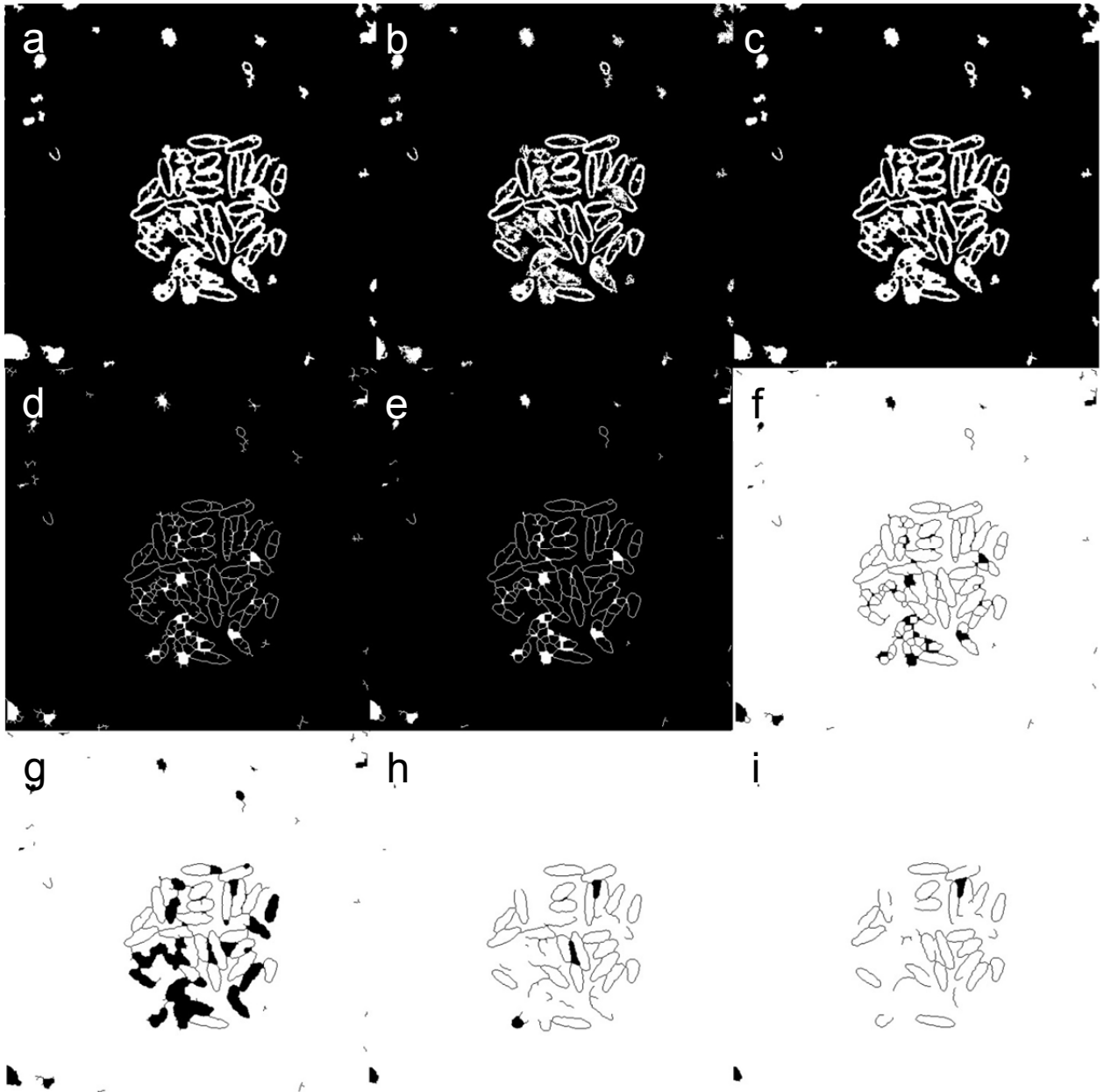
251 The next macro is called "clear body outliner" because the outlines produced are based on
252 image thresholding which target the white translucent area of the organism.

- 253 2. **Clear Body Outliner Preprocessing** (Macro: *schisto94_n_master*) (Figure 2) (53 operations
254 per image)
- 255 a. Transform FFC image with transform filter = local arithmetic (Macro: *schisto94_n_1950*):
 - 256 i. `sel(src<1950,4095,0);`
 - 257 b. Transform result from step "2.a" with transform filter = sieve (binary), retain objects > 500
258 μm^2
 - 259 c. Transform result from step "2.b" with transform filter = closing (binary), kernel = 3
 - 260 d. Transform result from step "2.c" with transform filter = thinning, passes = 3
 - 261 e. Transform result from step "2.d" with transform filter = pruning, passes = 3
 - 262 f. Transform result from step "2.e" with transform filter = inversion
 - 263 g. Transform result from step "2.f" with transform filter = sieve (binary), retain objects >
264 $2600 \mu\text{m}^2$
 - 265 h. Repeat steps "2.a" through "2.g" with following code for step "2.a", (Macro:
266 *schisto94_n_1800*):
 - 267 i. `sel(src<1800,4095,0);`
 - 268 i. Repeat steps "2.a" through "2.g" with following code for step "2.a", (Macro:
269 *schisto94_n_1700*):
 - 270 i. `sel(src<1700,4095,0);`
 - 271 j. Reset a channel with transform filter = local arithmetic
 - 272 i. `src = 0;`
 - 273 k. Transform result from "Macro: *schisto94_n_1950*" with transform filter = dilation (binary),
274 kernel = 3
 - 275 l. Apply a transform point operation = arithmetic (two src) where source1 = result from
276 threshold "Macro: *schisto94_n_1950*" and source2 = result from step "2.k".
 - 277 i. `src2-src1;`
 - 278 m. Apply a transform point operation = arithmetic (two src) where source1 = result from step
279 "2.j" and source2 = result from step "2.l". The result is added to the channel used in step
280 "j".
 - 281 i. `src2+src1;`
 - 282 n. Repeat steps "2.k" through "2.m" with result from "Macro: *schisto94_n_1800*".
 - 283 o. Repeat steps "2.k" through "2.m" with result from "Macro: *schisto94_n_1700*".
 - 284 p. Transform merge result (channel in step "j") with transform filter = inversion

- 285 q. Transform result from step "2.p" with transform filter = sieve (binary), retain objects > 100
286 μm^2
- 287 r. Transform result from step "2.q" with transform filter = inversion
- 288 s. Transform result from step "2.r" with transform filter = erosion, kernel = 3
- 289 t. Transform result from step "2.s" with transform filter = sieve (binary), retain objects > 100
290 μm^2
- 291 u. Transform result from step "2.t" with transform filter = pruning, passes = 3
- 292 v. Apply a transform point operation = arithmetic (two src) where source1 = result from step
293 "2.q" and source2 = result from step "2.u".
- 294 i. `src2+src1;`
- 295 w. Apply a transform point operation = arithmetic (two src) where source1 = result from step
296 "2.v" and source2 = result from step "1.h".
- 297 i. `sel(src1==4095,src2,0);`

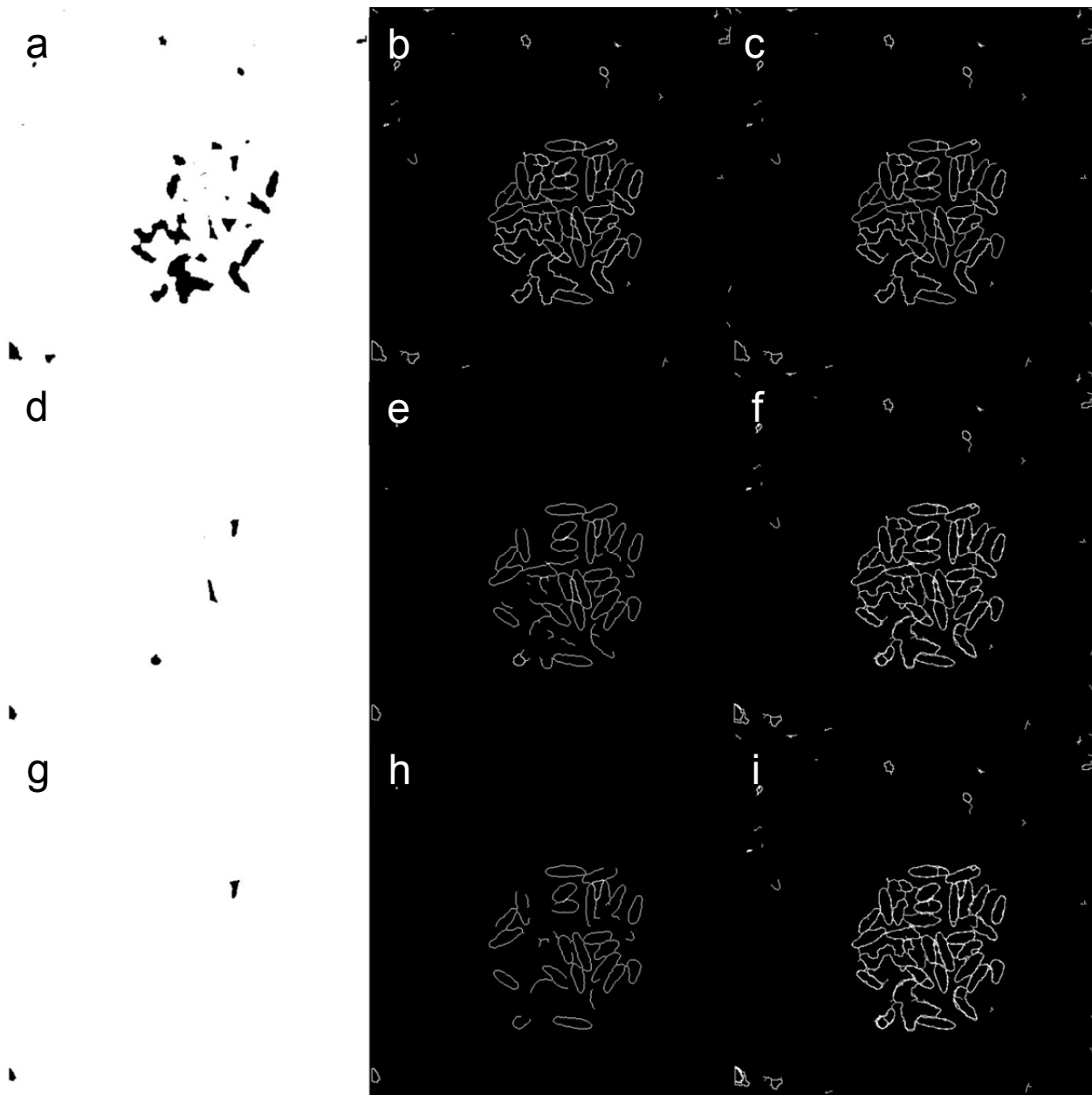
298 Steps "2.a" through "2.i" generate the preliminary target data for threshold1 to threshold3.
299 **(Figure 2A)** The refinement of this preliminary data and consolidation into a fourth target begins with
300 step "2.j". **(Figure 2B)** The fourth target is based on a merge of the data from the three thresholds. The
301 resulting outline will have extra objects produced by the intersections. The extra objects are filtered to
302 reduce complexity of the merged result and this process starts with step "2.p". **(Figure 3B)** In addition,
303 the merge result represents all possible objects all clear body target sets and these results are used to
304 patch holes in the results from threshold 1 to 3. A complete set of overlapping objects is a requirement
305 for target linking.

306
307
308
309
310



311
 312
 313
 314
 315
 316
 317
 318
 319
 320
 321

Figure 2A, Clear body workflow for thresholds 1 to 3. Panels “a” through “g” describe the clear body workflow for threshold1 (“Macro: *schisto94_n_1950*”). a) binarization of the flat field corrected image, b) sieve to remove small objects, c) closing to close gaps, d) thinning to reduce outline to a skeleton, e) pruning to prune back branches, f) inversion, g) sieve to retain large objects (this is the threshold1 “Macro: *schisto94_n_1950*” result), h) threshold2 “Macro: *schisto94_n_1800*” result, i) threshold3 “Macro: *schisto94_n_1700*” result.

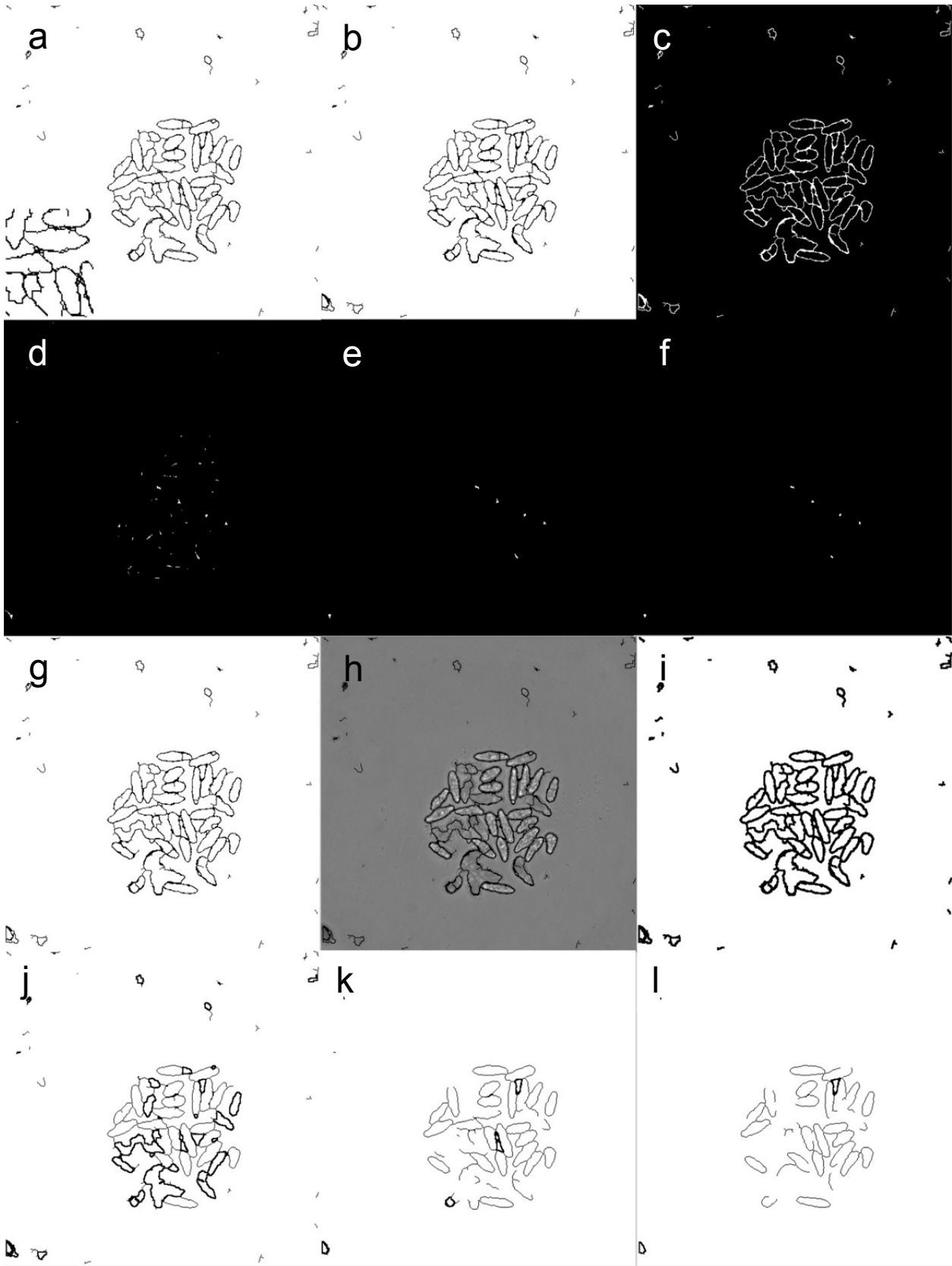


322

323 **Figure 2B, Merging thresholds 1 to 3 into the fourth target set.** Some targets, seen as black blobs
 324 in panel “a,d,g”, are discovered through the negative of the clear body workflow. Panel series “a,b,c”,
 325 “d,e,f”, and “g,h,i” (continues threshold 1,2,3 respectively) show three steps: 1) dilation of the result to
 326 expand the white area and erode the black blobs, 2) subtraction of the result from the dilation which
 327 adds black blobs as outlines to our set of outlines, 3) addition of the updated result to the merge
 328 channel. As we work through the second and third series, additional data is added to the merge
 329 channel until we have a rough merge result in panel “i”.

330

331



332
333

334 **Figure 2C, Refining merge result and preparing for target linking.** The merge result has tiny little
335 objects around the perimeter of the large objects which are produced from the intersection of three sets
336 of outlines from thresholds 1 to 3. These small objects are filtered and added back to the image if
337 passed (panel “a” to “g”). The finished merge result in panel “g” is assigned pixel values from the flat-
338 field corrected image (panel “h”). The merge result is eroded to provide objects that can patch the black
339 spaces (a requirement for target linking) in the images for the results for threshold 1 to 3. These
340 operations are shown in panels “i” to “l”. a) inversion of the merge result with a zoomed-in region
341 shown in the left corner to show the tiny little objects, b) sieve to remove small objects, c) inversion, d)
342 erosion e) sieve to remove small objects, f) prune branches, g) add the result from panel “f” to the result
343 from panel “b”, h) assign the pixel values from the flat field corrected image to any non-zero pixels in
344 panel “g”, i) erode the result from panel “g”, j) add the result from “j” to the result from “Fig2A.g”, k) add
345 the result from “j” to the result from “Fig2A.h”, l) add the result from “j” to the result from “Fig2A.i”.

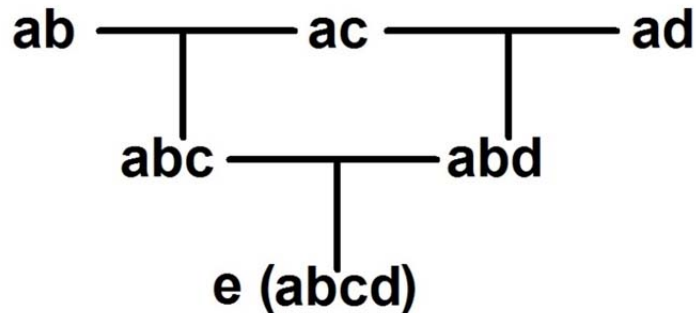
346

347 The merge result and results for threshold 1 to 3 are segmented using intensity segmentation
348 with a minimum threshold of 1.00 and a maximum threshold of 4095.00. These settings select all non-
349 zero pixels. The outlines of the objects produced by the preprocessing macro have pixel values of zero.
350 The merge result segmentation has additional post processing steps which use sieve (binary) to retain
351 objects between 1500 μm^2 and 50,000 μm^2 and border object removal to remove any objects within
352 5 pixels of the image border. Results from threshold 1 to 3 do not use additional post processing steps
353 to remove objects as this could remove objects needed for target linking.

354

355 Target linking uses object overlap from different images to determine which objects should be
356 analyzed as a group. Target linking removes objects that do not overlap between all images. Target
357 linking simplifies reporting by putting all feature data for each object found across four images on one
358 row. To make the linking schema easier to read, the four target sets (merge, threshold1, threshold2,
359 threshold3) are named “a”, “b”, “c”, “d”, respectively. Set “a” is linked to set “b”, “c”, and “d” using a “one
360 to one link” to form links “ab”, “ac”, and “ad”. An object in set “a” must be within 75% of the object it is
361 linking to otherwise the link is for those two objects are rejected. Link “ab” and “ac” are joined into link
362 “abc” using a “composed one to one link”. Link “ab” and “ad” are joined into link “abd” using a
363 “composed one to one link”. Link “abc” and “abd” are joined into link “abcd” (which was renamed to “e”)
364 using a “composed one to one link”. (**Figure 2D**)

a (merge), b (thresh1), c (thresh2), d (thresh3)



365
366
367

368 **Figure 2D, Target linking schematic.** The target sets are represented by letters “a”, “b”, “c”, and “d”
369 with “a” representing the merge data. The merge data contains all possible objects and is the root data
370 that links to “b”, “c”, and “d” forming “ab”, “ac”, and “ad” on the first row. “Composed one to one linking”
371 is used to link “ab” and “ac” using “matching path” data from “a” to form “abc”. “Composed one to one
372 linking” is used to link “ab” and “ad” using “matching path” data from “a” to form “abd”. “Composed one
373 to one linking” is used to link “abc” and “abd” using “matching path” data from “ab” to form “abcd” which
374 is renamed to “e”. Target set “e” contains all the linking data that relates objects found at similar
375 positions across data sets “a”, “b”, “c”, and “d”.

376

377 The next macro is called “tegument outliner” because the outlines produced are based on image
378 thresholding which target the tegument of the organism.

379

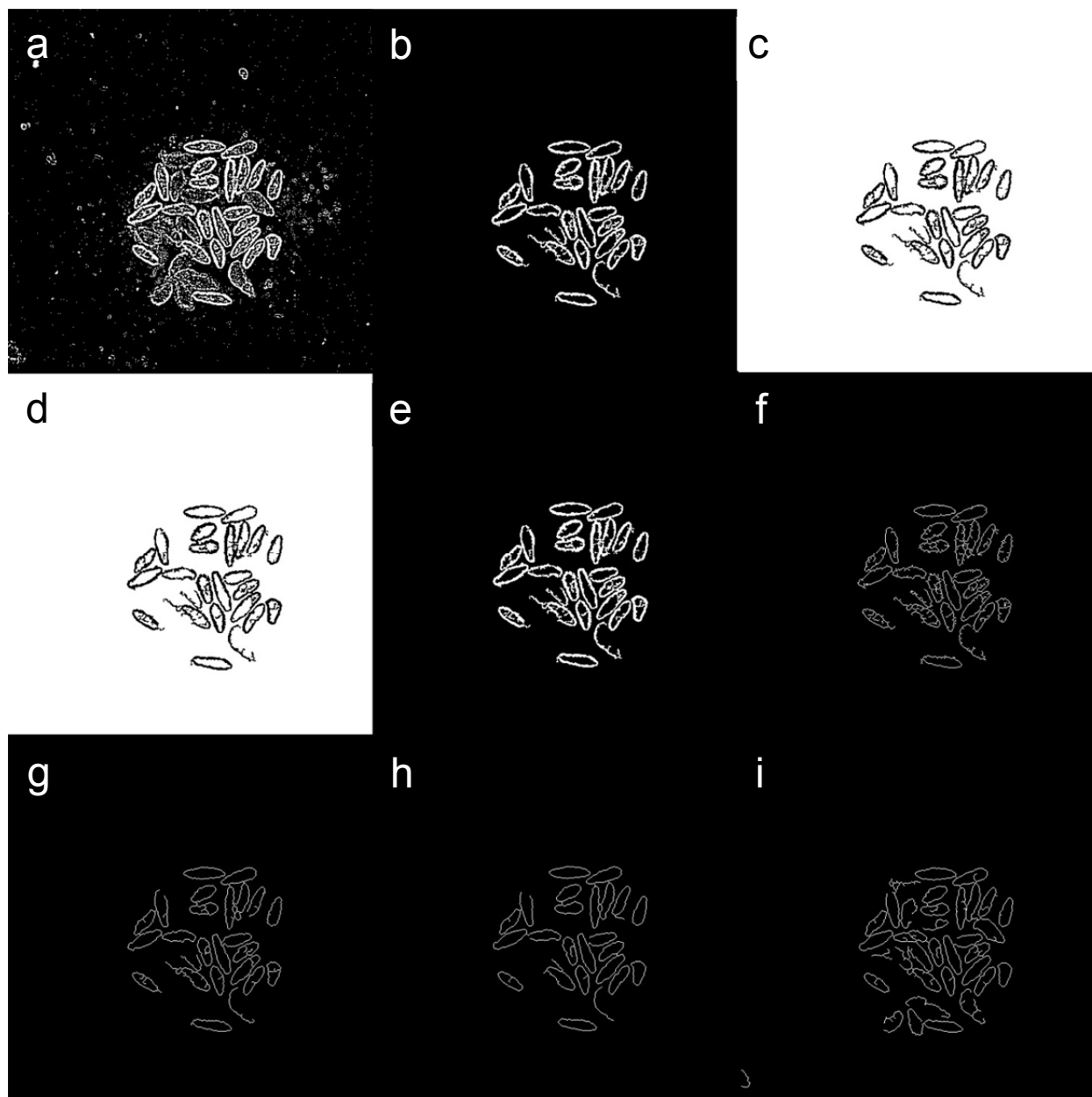
380 3. **Tegument Outliner Preprocessing** (Macro: *schisto94_g_master*) (**Figure 3**) (49 operations
381 per image)

- 382 a. Transform FFC image with transform filter = median, (Macro: *schisto94_g_med1_97*),
383 kernel = (do not apply transform)
- 384 b. Transform result from step “3.a” with local arithmetic (Macro: *schisto94_g_med1_97*):
385 i. kernel = 5;
386 ii. `sel(src<0.97*I Ave,4095,0);`
- 387 c. Transform result from step “3.a” with transform filter = sieve (binary), retain objects >
388 1500 μm^2
- 389 d. Transform result from step “3.b” with transform filter = inversion
- 390 e. Transform result from step “3.c” with transform filter = sieve (binary), retain objects > 100
391 μm^2
- 392 f. Transform result from step “3.b” with transform filter = inversion
- 393 g. Transform result from step “3.c” with transform filter = thinning, passes = 3
- 394 h. Transform result from step “3.d” with transform filter = pruning, passes = 3

- 395 i. Repeat steps “3.a” through “3.h” with following setting for step “3.a”, (Macro:
 396 *schisto94_g_med3_97*), kernel = 3 **AND** with the following code for step “3.b”, (Macro:
 397 *schisto94_g_med3_97*):
 398 i. kernel = 5;
 399 ii. sel(src<0.97*I_{Ave},4095,0);
- 400 j. Repeat steps “3.a” through “3.h” with following setting for step “3.a”, (Macro:
 401 *schisto94_g_med3_99*), kernel = 3 **AND** with the following code for step “3.b”, (Macro:
 402 *schisto94_g_med3_99*):
 403 i. kernel = 5;
 404 ii. sel(src<0.99*I_{Ave},4095,0);
- 405 k. Reset a channel with transform filter = local arithmetic
 406 i. src = 0;
- 407 l. Apply a transform point operation = arithmetic (two src) where source1 = result from
 408 “Macro: *schisto94_g_med1_97*” and source2 = result from step “3.k”. The result is added
 409 to the channel used in step “3.k”.
 410 i. src2+src1;
- 411 m. Repeat step “2.l” with source1 = result from “Macro: *schisto94_g_med3_97*”.
- 412 n. Repeat step “2.l” with source1 = result from “Macro: *schisto94_g_med3_99*”.
- 413 o. Transform merge result (channel in step “k”) with transform filter = inversion
- 414 p. Transform result from step “3.o” with transform filter = sieve (binary), retain objects > 100
 415 μm^2
- 416 q. Transform result from step “3.p” with transform filter = inversion
- 417 r. Transform result from step “3.q” with transform filter = erosion, kernel = 3
- 418 s. Transform result from step “3.r” with transform filter = sieve (binary), retain objects > 100
 419 μm^2
- 420 t. Transform result from step “3.s” with transform filter = pruning, passes = 3
- 421 u. Apply a transform point operation = arithmetic (two src) where source1 = result from step
 422 “3.p” and source2 = result from step “3.t”.
 423 i. src2+src1;
- 424 v. Apply a transform point operation = arithmetic (two src) where source1 = result from step
 425 “3.u” and source2 = result from step “1.h”.
 426 i. sel(src1==4095,src2,0);
- 427 w. Transform result from “Macro: *schisto94_g_med1_97*” with transform filter = inversion
- 428 x. Transform result from “Macro: *schisto94_g_med3_97*” with transform filter = inversion
- 429 y. Transform result from “Macro: *schisto94_g_med3_99*” with transform filter = inversion

430
 431

432 Steps “3.a” through “3.j” generate the preliminary target data for threshold1 to threshold3. (**Figure 3A**)
 433 The refinement of this preliminary data and consolidation into a fourth target begins with step “3.k”.
 434 (**Figure 3B**) The fourth target is based on a merge of the data from the three thresholds. The resulting
 435 outline will have extra objects produced by the intersections. The extra objects are filtered to reduce
 436 complexity of the merged result and this process starts with step “3.o”. (**Figure 3B**) In addition, the
 437 merge result represents all possible objects for all tegument outliner target sets. Steps “3.w” through
 438 “3.y” invert the results in preparation for segmentation.



440

441

442

443

444

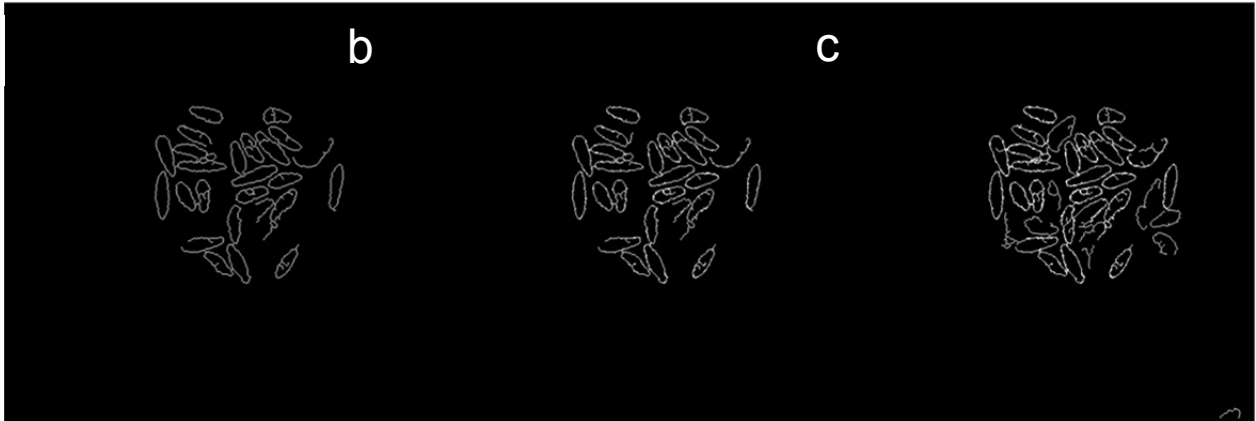
445

446

447

448

Figure 3A, Tegument outliner workflow for thresholds 1 to 3. Panels “a” through “g” describe the tegument outliner workflow for threshold1 (“Macro: *schisto94_g_med1_97*”). a) binarization of the flat field corrected image, b) sieve to remove small objects, c) inversion, d) sieve to remove small objects, e) inversion, f) thinning to reduce outline to a skeleton, g) pruning to prune back branches (this is the “Macro: *schisto94_g_med1_97*” result), h) threshold2 “Macro: *schisto94_g_med3_97*” result, i) threshold3 “Macro: *schisto94_g_med3_99*” result

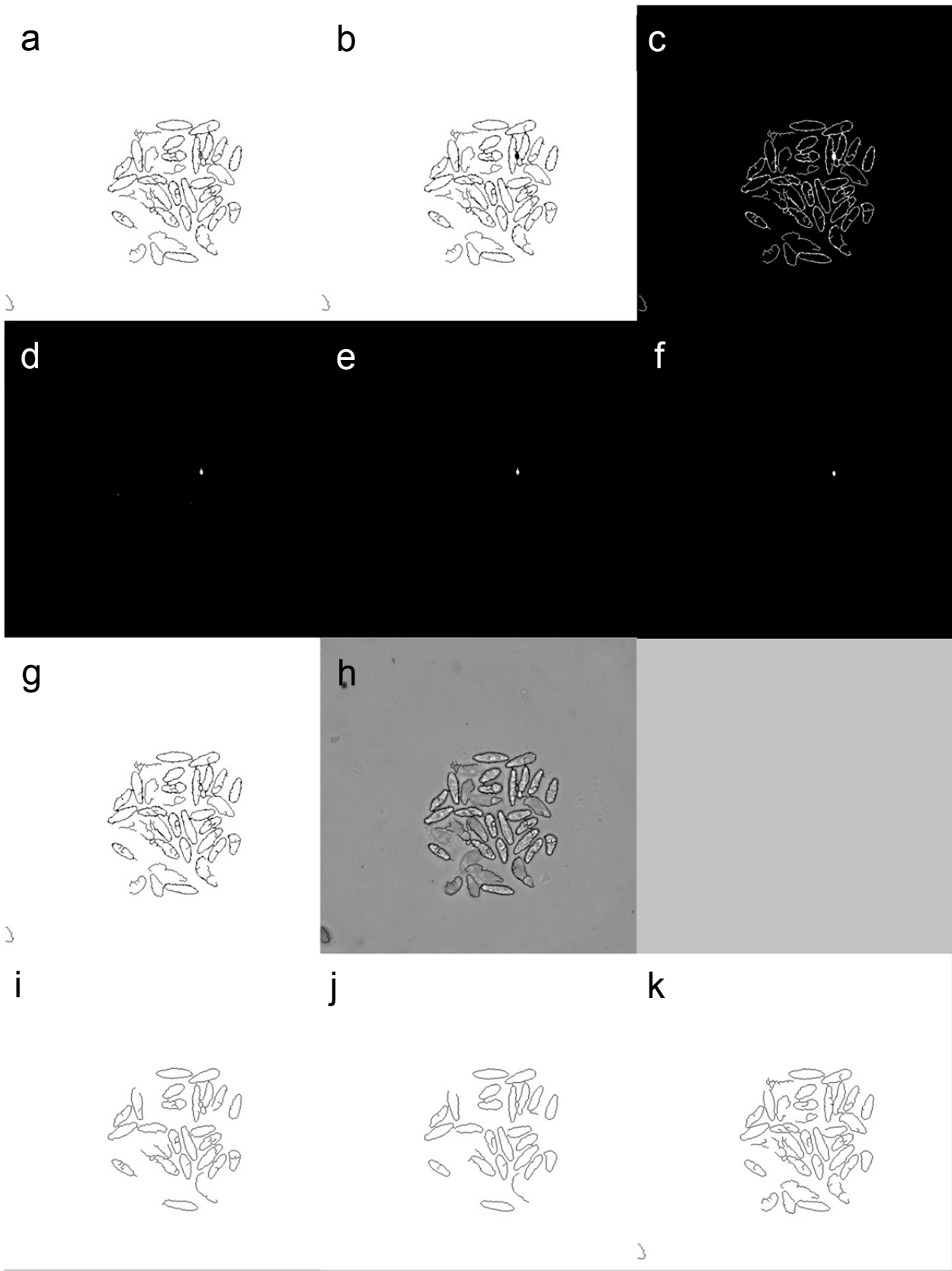


449
 450
 451
 452
 453
 454
 455
 456
 457
 458
 459
 460
 461
 462
 463
 464
 465
 466
 467
 468
 469
 470
 471
 472
 473
 474
 475
 476
 477
 478

Figure 3B, Merging thresholds 1 to 3 into the fourth target set. The results from each threshold are progressively added together into a rough merge result. a) threshold 1 result, b) threshold 1 and 2 results added together, c) threshold results 1, 2, and 3 added together.

The merge result and results for threshold 1 to 3 are segmented using intensity segmentation with a minimum threshold of 1.00 and a maximum threshold of 4095.00. These settings select all non-zero pixels. The outlines of the objects produced by the preprocessing macro have pixel values of zero. The merge result segmentation has additional post processing steps which use sieve (binary) to retain objects between 1500 μm^2 and 50,000 μm^2 and border object removal to remove any objects within 5 pixels of the image border. Results from threshold 1 to 3 do not use additional post processing steps to remove objects as this could remove objects needed for target linking.

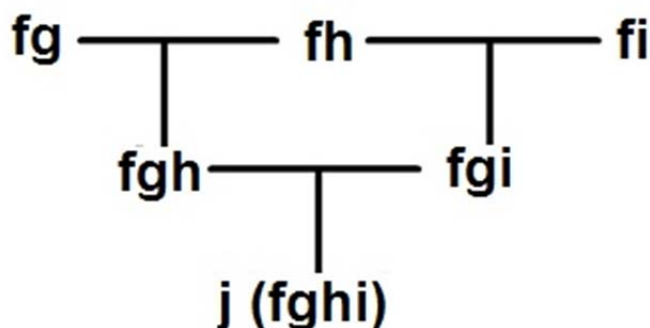
Target linking uses object overlap from different images to determine which objects should be analyzed as a group. Target linking removes objects that do not overlap between all images. Target linking simplifies reporting by putting all feature data for each object found across four images on one row. To make the linking schema easier to read, the four target sets (merge, threshold1, threshold2, threshold3) are named “f”, “g”, “h”, “i”, respectively. Set “f” is linked to set “g”, “h”, and “i” using a “one to one link” to form links “fg”, “fh”, and “fi”. An object in set “f” must be within 75% of the object it is linking to otherwise the link is for those two objects are rejected. Link “fg” and “fh” are joined into link “fgh” using a “composed one to one link”. Link “fg” and “fi” are joined into link “fgi” using a “composed one to one link”. Link “fgh” and “fgi” are joined into link “fghi” (which was renamed to “j”) using a “composed one to one link”. **(Figure 3D)**



479
480

481 **Figure 3C, Refining merge result and preparing for target linking.** The merge result has tiny little
 482 objects around the perimeter of the large objects which are produced from the intersection of three sets
 483 of outlines from thresholds 1 to 3. These small objects are filtered and added back to the image if
 484 passed (panel “a” to “g”). The finished merge result in panel “g” is assigned pixel values from the flat-
 485 field corrected image (panel “h”). The final results for the three sets of outlines from thresholds 1 to 3
 486 are shown in panels “i” to “k” respectively. a) inversion of the merge result, b) sieve to remove small
 487 objects, c) inversion, d) erosion e) sieve to remove small objects, f) prune branches, g) add the result
 488 from panel “f” to the result from panel “b”, h) assign the pixel values from the flat field corrected image
 489 to any non-zero pixels in panel “g”, i) inversion of “Fig2A.g”, j) inversion of “Fig2A.h”, k) inversion of
 490 “Fig2A.i”

f (merge), g (thresh1), h (thresh2), i (thresh3)



491
 492
 493

494 **Figure 3D, Target linking schematic.** The target sets are represented by letters “f”, “g”, “h”, and “i”
 495 with “f” representing the merge data. The merge data contains all possible objects and is the root data
 496 that links to “g”, “h”, and “i” forming “fg”, “fh”, and “fi” on the first row. “Composed one to one linking” is
 497 used to link “fg” and “fh” using “matching path” data from “f” to form “fgh”. “Composed one to one
 498 linking” is used to link “fg” and “fi” using “matching path” data from “f” to form “fgi”. “Composed one to
 499 one linking” is used to link “fgh” and “fgi” using “matching path” data from “fg” to form “fghi” which is
 500 renamed to “j”. Target set “j” contains all the linking data that relates objects found at similar positions
 501 across data sets “f”, “g”, “h”, and “i”.

502

4. Dark Body Outliner Preprocessing (Macro: *schisto94_d_master*) (Figure 4)

- 503 a. Reset a channel with transform filter = local arithmetic
 - 504 i. src = 0; (ch15)
- 505 b. (Macro: *schisto94_d_2050*), Transform FFC image with local arithmetic
 - 506 i. sel(src<2050,4095,0)
- 507 c. Transform result from step “4.b” with transform filter = sieve (binary), retain objects > 250
 508 μm^2
- 509 d. Transform result from step “4.c” with transform filter = inversion
- 510 e. Transform result from step “4.d” with local arithmetic

511

512 i. kernel = 3

513 ii. sel(src>2*I Ave,0,src)

514 f. Transform result from step “4.e” with transform filter = sieve (binary), retain objects >500

515 μm^2

516 g. Transform result from step “4.f” with transform filter = inversion (ch1)

517 h. Apply a transform point operation = copy result “4.g” (ch13... Macro: *schisto94_d_2050*

518 *RESULT*)

519 i. (Macro: *schisto94_d_fill*), Transform result from step “4.h” with local arithmetic

520 i. kernel =7

521 ii. sel(src>0,sel(src>I Ave,0,4095),0)

522 j. Transform result from step “4.i” with transform filter = sieve (binary), retain objects >

523 1500 μm^2

524 k. Transform result from step “4.j” with transform filter = dilation, kernel = 5 (ch14... Macro:

525 *schisto94_d_fill RESULT*)

526 l. Transform FFC image with local arithmetic, (Macro: *schisto94_d_1950*)

527 i. sel(src<1950,4095,0)

528 m. Transform result from step “4.l” with transform filter = sieve (binary), retain objects > 250

529 μm^2

530 n. Transform result from step “4.m” with transform filter = inversion

531 o. Transform result from step “4.n” with local arithmetic

532 i. kernel = 3

533 ii. sel(src>2*I Ave,0,src)

534 p. Transform result from step “4.o” with transform filter = sieve (binary), retain objects > 500

535 μm^2

536 q. Transform result from step “4.p” with transform filter = inversion (ch1)

537 r. Transform result from step “4.q” with local arithmetic, (Macro: *schisto94_c17*)

538 i. kernel = 17

539 ii. sel(src>0,sel(src==I Ave,4095,0),0)

540 s. Transform result from step “4.r” with transform filter = dilation, kernel = 3

541 t. Transform result from step “4.s” with transform filter = sieve (binary), retain objects <

542 2500 μm^2 (see step “4.r” for reason, kernel “seeds” will be small)

543 u. Apply a transform point operation = arithmetic (two src) where source1 = result from

544 “Macro: *schisto94_c17*” and source2 = result from step “4.a”. The result is added to the

545 channel used in step “4.a”. (ch15)

546 i. src2+src1;

547 v. Repeat step “4.r” through “4.v” with kernel = 15 from “Macro: *schisto94_c15*”.

548 w. Repeat step “4.r” through “4.v” with kernel = 13 from “Macro: *schisto94_c13*”.

549 x. Repeat step “4.l” through “4.x” with the following code for step “4.l” (Macro:

550 *schisto94_d_1450*).

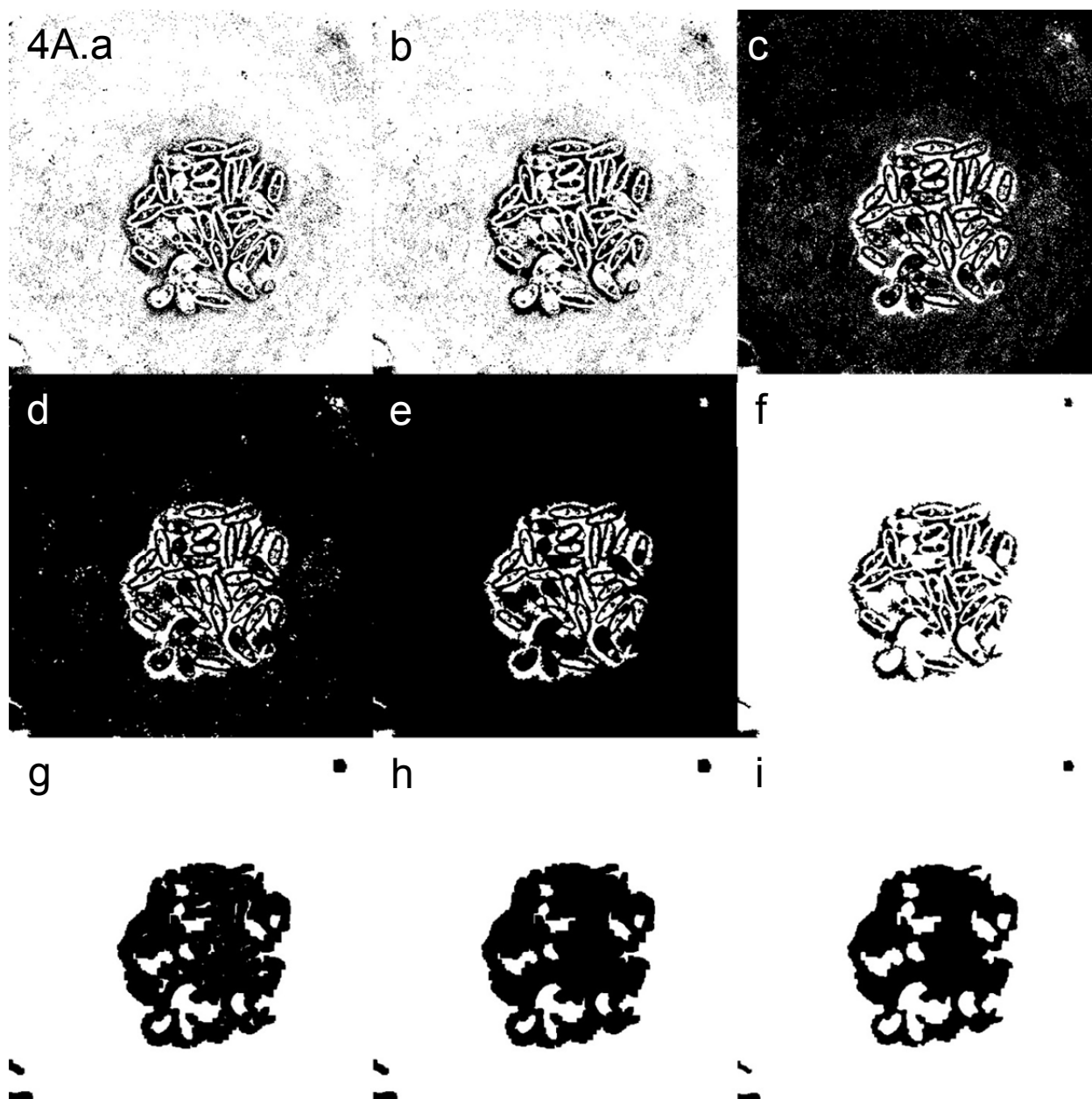
551 i. sel(src<1450,4095,0);

552 y. Repeat step “4.l” through “4.x” with the following code for step “4.l” (Macro:

553 *schisto94_d_1150*). After all loops completed this is: (ch15... Merge Seed *RESULT*)

554 i. sel(src<1150,4095,0);

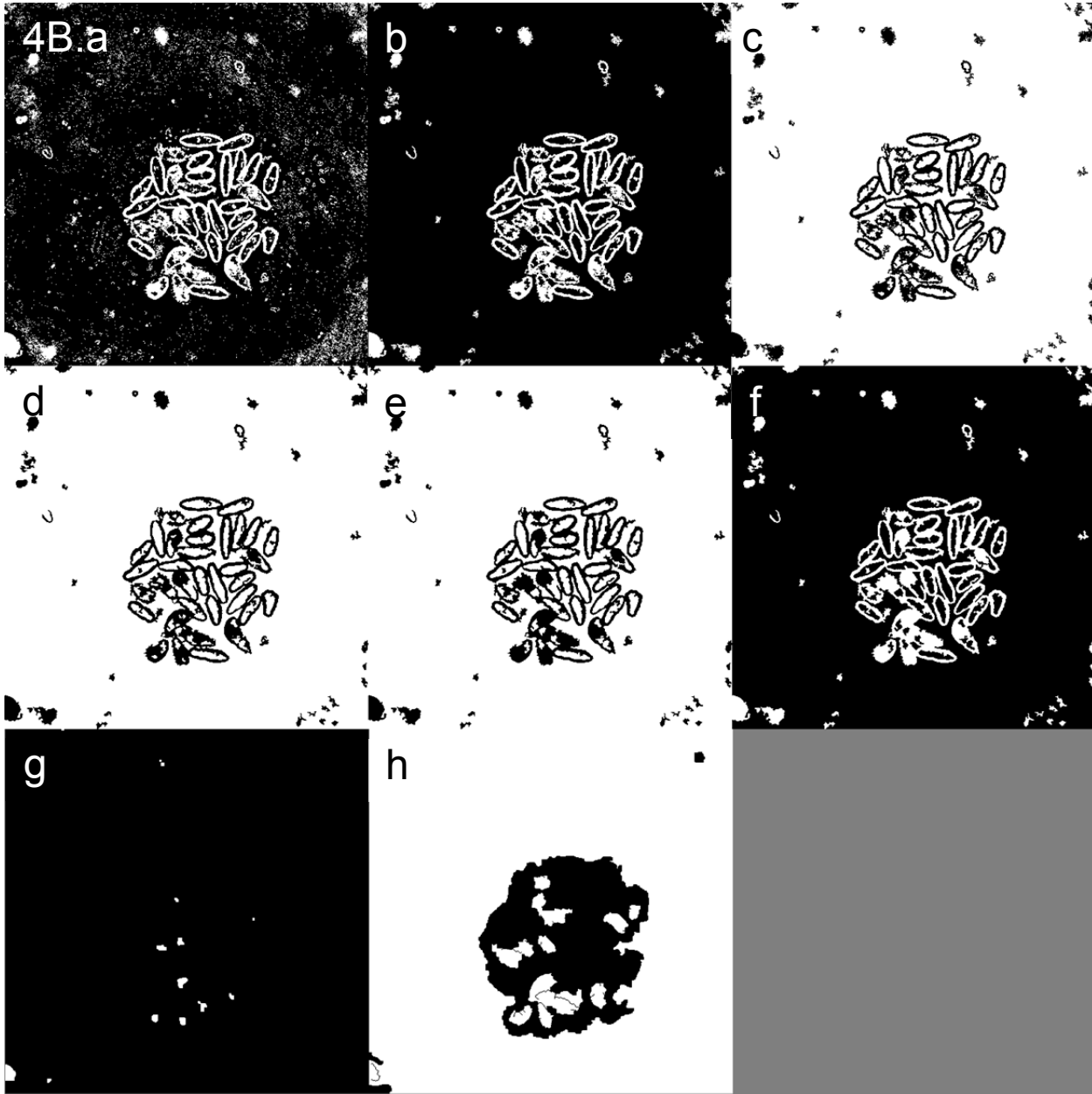
- 555 z. Apply a transform point operation = arithmetic (two src) where source1 = result from step
 556 "3.u" and source2 = result from step "4.k".
 557 i. `sel(src1<1,src1,src2);` (ch16... Macro: *schisto94_d_fill RESULT combined with*
 558 *the Tegument Outliner Merge Result*)
 559 aa. Transform result from step "4.aa" with transform filter = sieve (binary), retain objects >
 560 1500 μm^2 (ch16)
 561 bb. Apply a transform point operation = copy result "4.z" (ch1)
 562



563
 564

565 **Figure 4A, Dark body outliner part 1.** Steps "4.a" through "4.k". a) binarization, b) sieve to remove
 566 small objects, c) inversion, d) enhance dark body with local adaptive thresholding, e) sieve to remove
 567 small objects, f) inversion to get 1st target image (Macro: *schisto94_d_2050*), g) local arithmetic to

568 isolate dark bodies (white blobs), h) sieve to remove small objects, i) dilation to get 2nd target image
 569 (Macro: schisto94_d_fill)
 570
 571
 572



573
 574
 575 **Figure 4B, Dark body outliner part 2.** Steps “4.l” through “4.v”. (Macro: *schisto94_d_1950*). a)
 576 binarization, b) sieve to remove small objects, c) inversion, d) enhance dark body with local adaptive
 577 thresholding, e) sieve to remove small objects, f) inversion, g) dark body “seeds” generated after
 578 iterative processing to get 3rd target image (Macro: (see step 4.z)), h) Macro: *schisto94_d_fill* result
 579 “4.k” combined with the tegument outliner merge result “3.u” to get the 4th target set (4B.h).
 580

581 To detect dark bodies a variety of approaches were used. The image was scanned with varying
582 thresholds (density = 1950, 1450, 1150) and kernels (k = 13, 15, and 17) to generate “seeds” of
583 possible dark bodies. The “seed” target set (4B.g) is similar to previously discussed merge results for
584 clear body and tegument outliner in that available target across multiple treatments are represented by
585 a single object. Dark bodies are found (4A.f) by simply taking the inverse of previously described clear
586 body outlining methods. Rather than produce an outline, as with a clear body, dark bodies produce
587 large filled objects with the complication that these objects are sometimes surrounded by other outlines.
588 The surrounding outlines can be diminished to leave the larger dark bodies behind, but at a cost of
589 some distortion to the dark body shape (4A.i). Finally, the tegument outliner merge result (3C.g) is
590 combined with the result from Macro: *schisto94_d_fill* (4A.h) to separate touching objects (4B.h).

591
592 The four binarized dark body target images are transformed back to original FFC image values
593 with the following transform. Apply a transform point operation = arithmetic (two src) where source1 =
594 binarized target image and source2 = FFC image. Code = “sel(src1==4095,src2,0);”.

595
596 *Dark body “seed” segmentation (K)*

597
598 The “seed” objects (4B.g) are segmented with intensity segmentation where objects with a pixel
599 value > 0 are masked. The masks are post-processed with a sieve which removes objects less than
600 250 μm^2 .

601
602 *Dark body “fill” segmentation part I (L)*

603
604 The objects from the Macro: *schisto94_d_fill* result (4.k) are segmented with intensity
605 segmentation where objects with a pixel value > 0 are masked. Objects within 5 pixels from the border
606 are removed using “border object removal”. The remaining masks are further post-processed with
607 clump breaking using masks segmented in the *dark body “seed” segmentation* as seeds. The masks
608 are post-processed with a sieve which removes objects less greater than 50,000 μm^2 .

609
610 *Dark body “combo” segmentation (seed generation)*

611
612 The target image generated from Macro: *schisto94_d_fill* result “4.k” combined with the
613 tegument outliner merge result “3.u” are segmented with intensity segmentation where objects with a
614 pixel value > 0 are masked. The masks are post-processed with an erosion (kernel = 3) and a sieve
615 which removes objects less greater than 500 μm^2 .

616
617 *Dark body “fill” segmentation part II (N)*

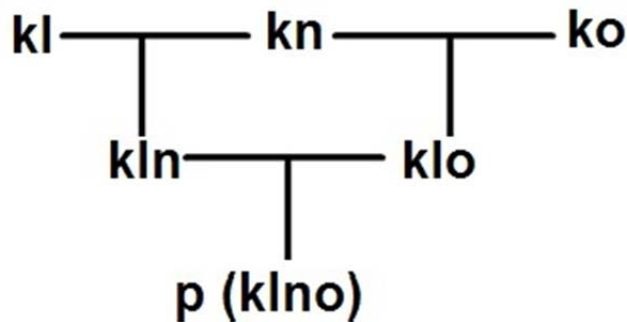
618
619 The objects from the Macro: *schisto94_d_fill* result (4.k) are segmented with intensity
620 segmentation where objects with a pixel value > 0 are masked. Objects within 5 pixels from the border
621 are removed using “border object removal”. Clump breaking is applied to the remaining masks with
622 masks segmented in the *dark body “combo” segmentation* as seeds. The masks are further post-
623 processed with watershed clump breaking and a sieve which removes objects less greater than 2,000
624 μm^2 .

625
626
627
628
629
630
631

Dark body “fill” segmentation part III (O)

The objects from the Macro: *schisto94_d_fill* result (4.k) are segmented with intensity segmentation where objects with a pixel value > 0 are masked. Objects within 5 pixels from the border are removed using “border object removal”. The masks are further post-processed with watershed clump breaking and a sieve which removes objects less greater than 2,000 μm^2 .

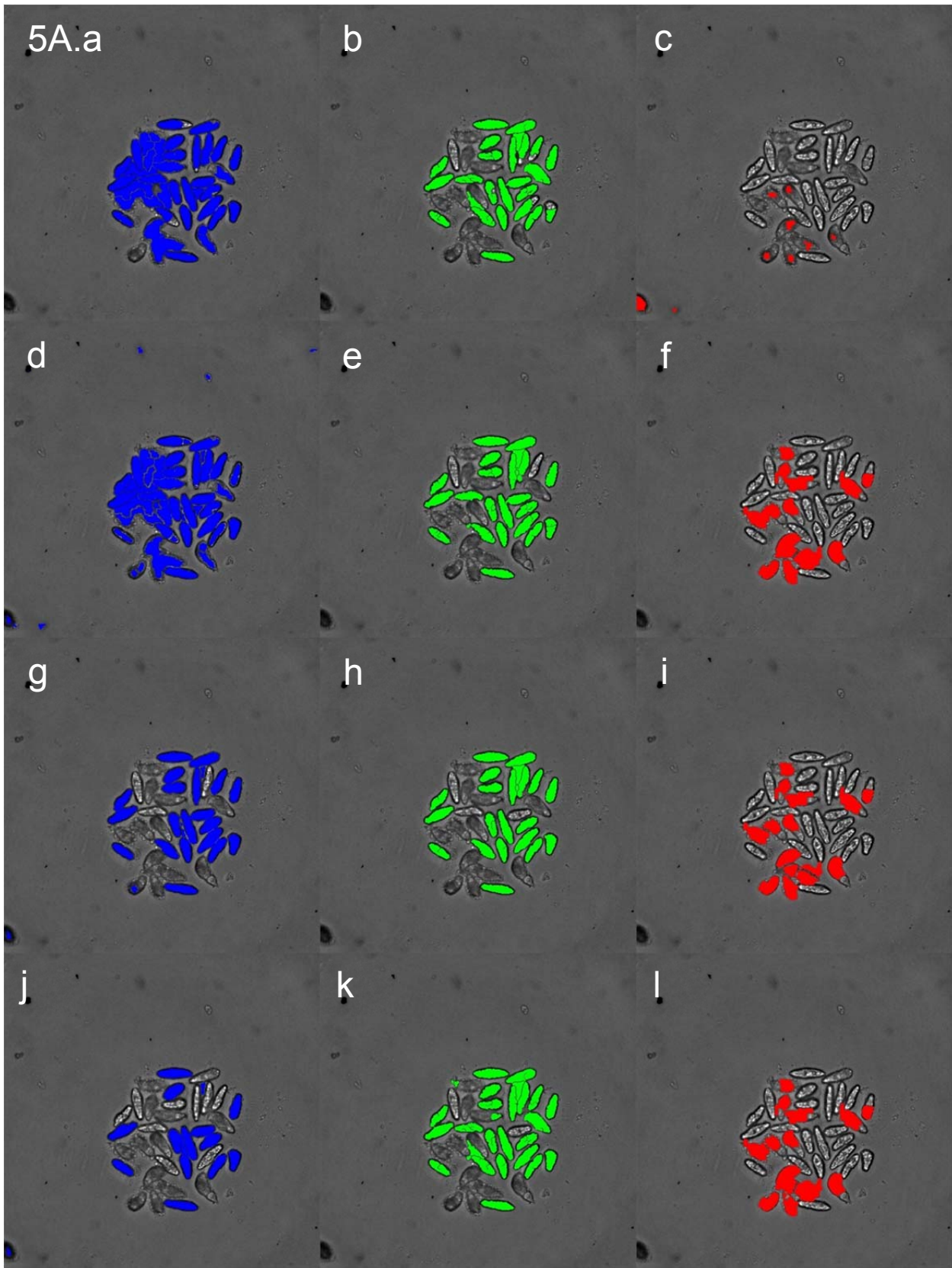
k (seed), l (fill part1), n (fill part 2), o (fill part3)



632
633
634
635
636
637
638
639
640
641
642
643
644
645

Figure 4D, Target linking schematic. The target sets are represented by letters “k”, “l”, “n”, and “o” with “k” representing the seed data. The merge data contains all possible objects and is the root data that links to “l”, “n”, and “o” forming “kl”, “kn”, and “ko” on the first row. “Composed one to one linking” is used to link “kl” and “kn” using “matching path” data from “k” to form “kln”. “Composed one to one linking” is used to link “kl” and “ko” using “matching path” data from “k” to form “klo”. “Composed one to one linking” is used to link “kln” and “klo” using “matching path” data from “kl” to form “klno” which is renamed to “p”. Target set “p” contains all the linking data that relates objects found at similar positions across data sets “k”, “l”, “n”, and “o”.

Figure 5A shows various masking results among the 12 target sets generated. It appears that “**Fig5A.a**” captured most of the objects using a clear body merge set. Missing, incomplete, joined, or broken masks have more or less complete counterparts found in other panels. In total, the 12 sets of masks form a more complete set of objects that any one set can provide alone.



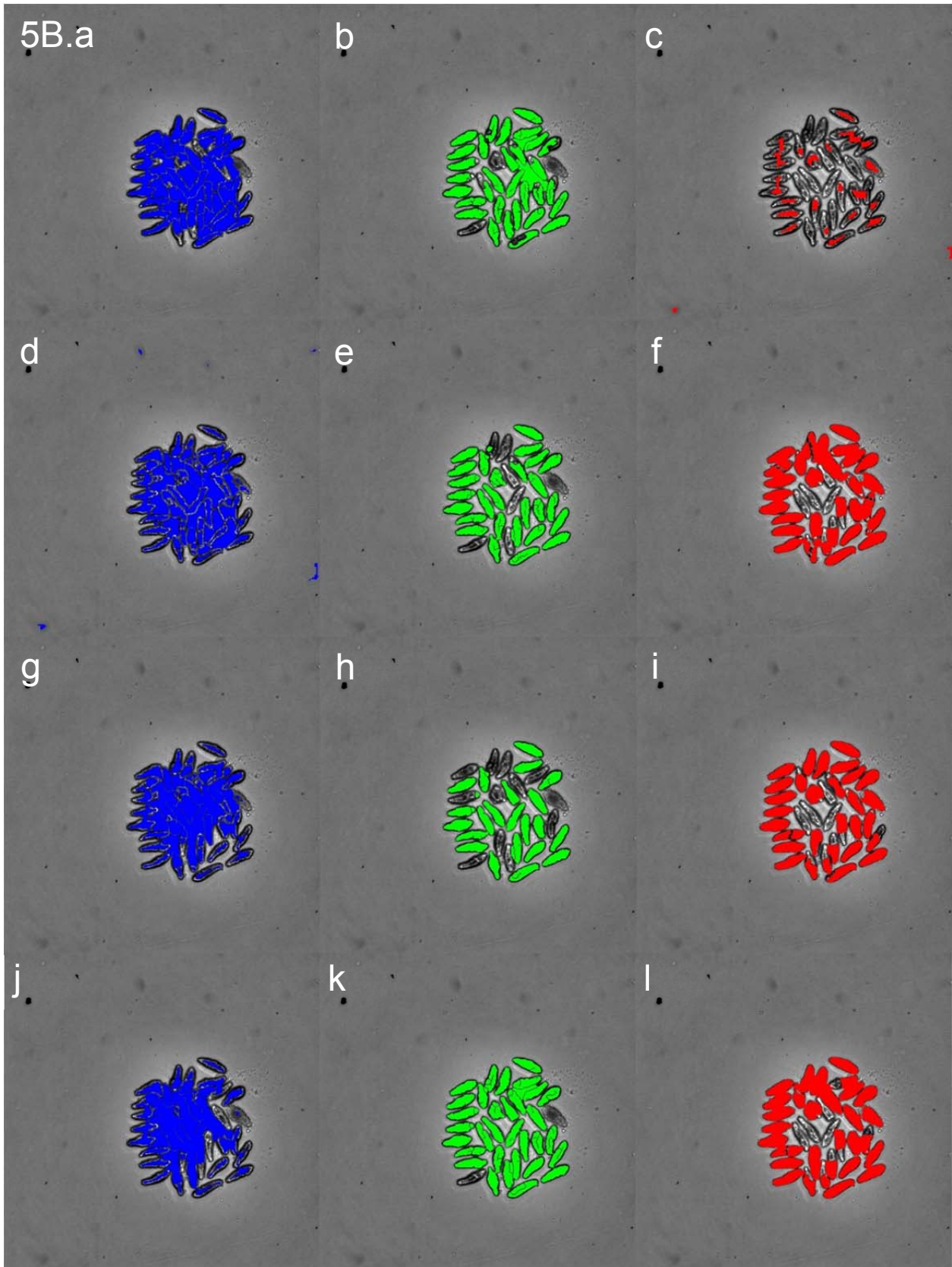
647 **Figure 5A, Target set masks for a mixed clear and dark body example.** Clear body targets are
648 shown in blue, tegument outliner targets are shown in green and dark body targets in red. The top row
649 of the figure show results from the merge data sets for clear body and tegument outliner with the
650 “seeds” from dark body shown in red. In subsequent rows, the binarization threshold becomes darker
651 for the blue clear body target set, increase in smoothing and decrease in stringency for outline
652 detection in green tegument outliner, and different clump breaking approaches using different seeds
653 shown in the red dark body target set. For the clear body set: a) merge set, d) threshold 1, g) threshold
654 2, j) threshold 3. For the tegument outline set: b) merge set, e) threshold 1, h) threshold 2, k) threshold
655 3. For the dark body target set: c) “seeds”, f) fill part 1, i) fill part 2, l) fill part 3.

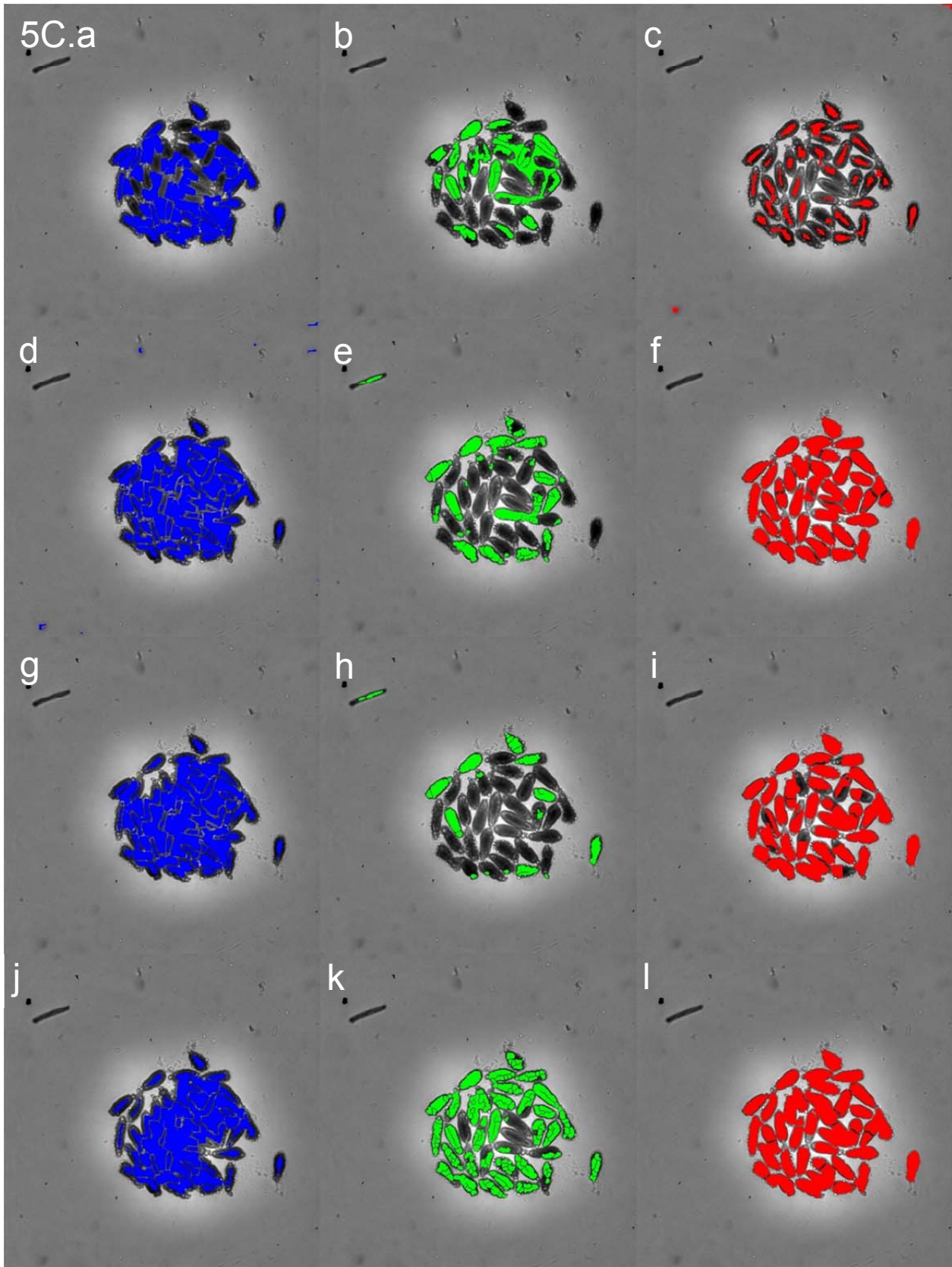
656
657 **Figure 5B** shows various masking results among the 12 target sets generated. It appears that
658 the clear body workflow captured most of the objects using a clear body merge set but most of the
659 masks are joined to other masks leading to a poor segmentation result. The dark body workflow
660 performs better but still suffers from objects that are masked together. The tegument outliner performed
661 the best in terms of finding individual objects with accurate masks. Missing, incomplete, joined, or
662 broken masks have more or less complete counterparts found in other panels. In total, the 12 sets of
663 masks form a more complete set of objects that any one set can provide alone.

664
665
666 **Figure 5C, Target set masks for dark body.** Clear body targets are shown in blue, tegument outliner
667 targets are shown in green and dark body targets in red. The top row of the figure show results from the
668 merge data sets for clear body and tegument outliner with the “seeds” from dark body shown in red. In
669 subsequent rows, the binarization threshold becomes darker for the blue clear body target set, increase
670 in smoothing and decrease in stringency for outline detection in green tegument outliner, and different
671 clump breaking approaches using different seeds shown in the red dark body target set. For the clear
672 body set: a) merge set, d) threshold 1, g) threshold 2, j) threshold 3. For the tegument outline set: b)
673 merge set, e) threshold 1, h) threshold 2, k) threshold 3. For the dark body target set: c) “seeds”, f) fill
674 part 1, i) fill part 2, l) fill part 3.

675
676 **Figure 5C** shows various masking results among the 12 target sets generated. It appears that the clear
677 body workflow captured most of the objects using a clear body merge set but most of the masks are
678 joined to other masks leading to a poor segmentation result. The tegument outliner workflow performs
679 better but still suffers from objects that are masked together or missing altogether. The dark body
680 workflow performed the best in terms of finding individual objects with accurate masks. Missing,
681 incomplete, joined, or broken masks have more or less complete counterparts found in other panels. In
682 total, the 12 sets of masks form a more complete set of objects that any one set can provide alone.

683
684
685
686
687





689
690

691

692 Features (area, length, color, etc) are recorded for every object in all 12 target sets with an IN
693 Cell Developer analysis time of about 5 hours per plate. The data is exported to a comma separated file
694 (CSV) typically weighing in at approximately 100 megabytes and containing more than 40 million data
695 points to describe 200,000 objects. Macro parameters can be easily modified to extend the range or
696 resolution of this approach, or even to adapt segmentation to different organisms.

697

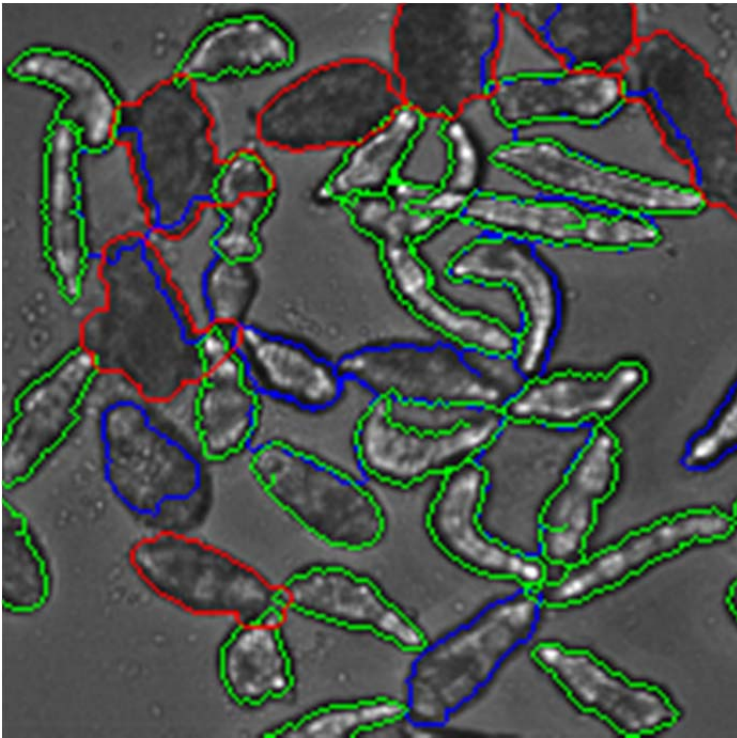
698 **Data Pre-Processing**

699

700 Before the data from IN Cell Developer can be analyzed and turned into descriptors for
701 database entry, the large data file requires treatment for the following:

702

- 703 1. Correct for segmentation feature offset (bias introduced from differences in segmentation)
- 704 2. Choose the best mask out of the twelve possible masks to represent the object. There may be
705 no best object if all fail to be within certain size limits.
- 706 3. Use organism-level and well-level data in both appearance and motion-based descriptors to
707 classify objects as either “clear body”, “dark body”, or non-organism objects. Non-organism
708 objects are removed from further analysis.



709

710 **Figure 6 Best mask to represent the object.** Image shows the best mask to represent the object from
711 the set of 12 possible masks. Blue outlines are derived from the clear body workflow, green outlines are
712 from the tegument outliner, and red outlines are from the dark body workflow.

713

713 **Choosing the Best Mask**

714

715 In the process of choosing the best mask, the objects are first filtered and reorganized. Objects
716 that are too small or too large are removed from analysis. The next step is to link objects within each
717 workflow by x and y position over time. Objects are linked to the coordinates of the last time-point or to
718 an average of all the previous time-points when there are gaps. The workflow that generated masks
719 with the most persistence over time was selected as the best series of masks to move forward with
720 analysis. In the case where workflows generated series with the same amount of persistence, the
721 series with the lower x,y variability over time was selected.

722

723 **Object Classification**

724

725 The object classifier uses organism-level data and well-level data to classify objects as clear
726 body, dark body, intra-body artifact, or inter-body artifact. First, the objects were linked through the
727 time-lapse images by x,y position. The time-linked objects were then used to generate feature
728 descriptors (such as mean, standard deviation) at both levels. Descriptors were then entered into
729 Model_1 to classify an object as a clear object or a dark object. Each additional level of classification
730 refines a part of the previous result. Model_2_Clear then classifies a clear object as a clear organism or
731 a clear non-organism (e.g. an object formed between organisms). Model_3_Clear then classifies a
732 clear organism as a complete clear organism or a partial clear organism (e.g. a partial masking of the
733 organism due to an internal boundary). Model_2_Dark and Model_3_Dark perform the same operations
734 but for the dark objects from Model_1.

735

- 736 1. Set objects in the first available time point as reference positions.
- 737 2. Set objects in the next available time points at test positions.
- 738 3. If a test position is less than $35 \mu\text{m}^2$ from a reference position than record a time linkage.
- 739 4. Set test positions as reference positions.
- 740 5. Repeat steps 2 through 4 until all time points have been processed.
- 741 6. Calculate mean and standard deviation at the organism level and at the well level.
- 742 7. Calculate the persistence at the organism level and at the well level. Persistence is the count of
743 time-linkages divided by the total number of time-lapse points for a given object. Objects with <
744 5% persistence are removed from analysis.
- 745 8. Classify an object as a clear object or a dark object (model_1: clear < 0.62)
 - 746 a. Classify a clear object as a clear organism or a clear non-organism object
747 (model_2_clear: $0.75 < \text{non-organism} < 2.5$)
 - 748 i. Classify a clear organism as a complete clear organism or a partial clear
749 organism (model_3_clear: $0.48 < \text{partial} < 2.5$)
 - 750 b. Classify a dark object as a dark organism or a dark non-organism object (model_2_dark:
751 $0.8 < \text{non-organism} < 2.5$)
 - 752 i. Classify a dark organism as a complete dark organism or a partial dark organism
753 (model_3_dark: $0.54 < \text{partial} < 2.5$)
- 754 9. Write data for clear and dark complete organisms to a new CSV file.

755 **Model_1**

756 n(0) = percent persistence (organism level); n(1) = density – levels mean (organism level); n(2) = SD –
757 levels mean (organism level); n(3) = form factor mean (well level); n(4) = density – levels mean (well
758 level)

759 $R1 = 18.25203487215 + 1.161068183069 * n(0) + 0.75542095675251 * n(1) + -0.68305180301445 * n(2) +$
760 $-1781.6761055724 * n(3) + -0.045006141550507 * n(4) + 3.2365931882399E-04 * n(0) * n(1) +$
761 $4.1740004117079E-04 * n(0) * n(2) + -4.6310458346469 * n(0) * n(3) + -5.7890475949427E-04 * n(0) * n(4) +$
762 $-9.8420513221299E-05 * n(1) * n(2) + -2.1884015714641 * n(1) * n(3) + -2.7848992087403E-04$
763 $* n(1) * n(4)$

764 $R2 = 1.3369398769791 * n(2) * n(3) + 8.9582262126079E-04 * n(2) * n(4) + 3.3329037457293 * n(3) * n(4) +$
765 $-1.8232199977951E-03 * n(0) ^ 2 + -9.4790505473488E-05 * n(1) ^ 2 + -2.2142492356085E-04 * n(2) ^ 2 +$
766 $2134.9935522591 * n(3) ^ 2 + -4.7102296313054E-04 * n(4) ^ 2 + 1.2266056885224E-06 * n(0) * n(1) * n(2) +$
767 $-9.2354913779362E-04 * n(0) * n(1) * n(3) + -1.6491057509021E-07 * n(0) * n(1) * n(4) +$
768 $1.5522216710331E-04 * n(0) * n(2) * n(3) + -8.2092941369132E-07 * n(0) * n(2) * n(4)$

769 $R3 = 2.9992856931552E-03 * n(0) * n(3) * n(4) + -3.5217569712729E-04 * n(1) * n(2) * n(3) +$
770 $6.5107500960996E-08 * n(1) * n(2) * n(4) + 2.6791800633611E-04 * n(1) * n(3) * n(4) +$
771 $9.0380771936169E-04 * n(2) * n(3) * n(4) + 3.1247731735274E-06 * n(0) ^ 2 * n(2) +$
772 $5.6240376267275E-03 * n(0) ^ 2 * n(3) + -1.4549471230916E-06 * n(0) ^ 2 * n(4) +$
773 $7.2417177105256E-08 * n(0) * n(1) ^ 2 + -6.1772369143247E-07 * n(0) * n(2) ^ 2 + 3.781429940739 * n(0) * n(3) ^ 2 +$
774 $1.0418245071802E-07 * n(0) * n(4) ^ 2 + 1.0219248176663E-07 * n(1) ^ 2 * n(2)$

775 $R4 = 4.5564375868527E-04 * n(1) ^ 2 * n(3) + -3.2106682445134E-08 * n(1) ^ 2 * n(4) +$
776 $1.8650850919366E-07 * n(1) * n(2) ^ 2 + 1.9206238869076 * n(1) * n(3) ^ 2 + 1.1738445506832E-07 * n(1) * n(4) ^ 2 +$
777 $3.7442327867001E-05 * n(2) ^ 2 * n(3) + 3.1503030609951E-07 * n(2) ^ 2 * n(4) +$
778 $-0.24033752947827 * n(2) * n(3) ^ 2 + -4.3786761514222E-07 * n(2) * n(4) ^ 2 + -3.4671132225482 * n(3) ^ 2 * n(4) +$
779 $-6.8418530427196E-04 * n(3) * n(4) ^ 2 + 7.6446830499591E-06 * n(0) ^ 3 +$
780 $1.0108280682996E-08 * n(1) ^ 3$

781 $R5 = 1.2530435647321E-07 * n(2) ^ 3 + -682.50789300831 * n(3) ^ 3 + 2.3776592427786E-07 * n(4) ^ 3 +$
782 $-8.3535696931061E-07 * n(0) * n(1) * n(2) * n(3) + -1.5257479853204E-10 * n(0) * n(1) * n(2) * n(4) +$
783 $4.0724584996769E-07 * n(0) * n(1) * n(3) * n(4) + 4.604799340958E-07 * n(0) * n(2) * n(3) * n(4) +$
784 $-8.7746281304306E-10 * n(0) ^ 2 * n(2) ^ 2 + -3.3302009301847E-06 * n(0) ^ 2 * n(2) * n(3) +$
785 $4.756929644064E-10 * n(0) ^ 2 * n(2) * n(4) + -3.4228762882309E-03 * n(0) ^ 2 * n(3) ^ 2 +$
786 $6.5899847343375E-10 * n(0) ^ 2 * n(4) ^ 2 + -1.1829905701319E-10 * n(0) * n(1) ^ 2 * n(2)$

787 $R6 = -6.5159315821518E-08 * n(0) * n(1) ^ 2 * n(3) + 5.2720741951882E-04 * n(0) * n(1) * n(3) ^ 2 +$
788 $4.9534714604476E-07 * n(0) * n(2) ^ 2 * n(3) + 4.1269226932606E-10 * n(0) * n(2) ^ 2 * n(4) +$
789 $6.3407631003489E-04 * n(0) * n(2) * n(3) ^ 2 + 1.494970625121E-10 * n(0) * n(2) * n(4) ^ 2 +$
790 $1.6907505821672E-03 * n(0) * n(3) ^ 2 * n(4) + -5.1365605396076E-07 * n(0) * n(3) * n(4) ^ 2 +$
791 $-3.6155421452363E-11 * n(1) ^ 2 * n(2) ^ 2 + -4.8126433937627E-08 * n(1) ^ 2 * n(2) * n(3) +$
792 $-1.7625953726279E-11 * n(1) ^ 2 * n(2) * n(4) + -3.2351132584444E-04 * n(1) ^ 2 * n(3) ^ 2 +$
793 $7.9530874313422E-08 * n(1) ^ 2 * n(3) * n(4)$

$$\begin{aligned}
794 \quad R7 = & -2.669952144001E-11 * n(1) ^ 2 * n(4) ^ 2 + 1.4503329430718E-07 * n(1) * n(2) ^ 2 * n(3) + \\
795 \quad & 1.4365500750249E-10 * n(1) * n(2) ^ 2 * n(4) + 4.2874540494959E-04 * n(1) * n(2) * n(3) ^ 2 + - \\
796 \quad & 3.6294914163709E-11 * n(1) * n(2) * n(4) ^ 2 + -3.3805927443037E-04 * n(2) ^ 2 * n(3) ^ 2 + - \\
797 \quad & 1.4210910495358E-10 * n(2) ^ 2 * n(4) ^ 2 + 2.3003285709267E-07 * n(2) * n(3) * n(4) ^ 2 + \\
798 \quad & 4.9777029628825E-04 * n(3) ^ 2 * n(4) ^ 2 + 2.97760253571E-09 * n(0) ^ 3 * n(2) + - \\
799 \quad & 4.3123259790407E-09 * n(0) ^ 3 * n(4) + 2.8293207850737E-11 * n(0) * n(1) ^ 3 + - \\
800 \quad & 2.6346389605596E-10 * n(0) * n(2) ^ 3
\end{aligned}$$

$$\begin{aligned}
801 \quad R8 = & -0.67260141510363 * n(0) * n(3) ^ 3 + 1.8752589917427E-08 * n(1) ^ 3 * n(3) + \\
802 \quad & 3.5136792540332E-11 * n(1) ^ 3 * n(4) + -1.7714456049114E-11 * n(1) * n(2) ^ 3 + - \\
803 \quad & 0.46479901154684 * n(1) * n(3) ^ 3 + -3.4875673740552E-08 * n(2) ^ 3 * n(3) + -2.5841449832186E- \\
804 \quad & 11 * n(2) ^ 3 * n(4) + -0.22134015982785 * n(2) * n(3) ^ 3 + 8.7853677440858E-11 * n(2) * n(4) ^ 3 + \\
805 \quad & 0.86618600900044 * n(3) ^ 3 * n(4) + -9.5374757135764E-12 * n(1) ^ 4 + -3.6583886794751E-11 * \\
806 \quad & n(4) ^ 4 + 0
\end{aligned}$$

$$807 \quad \text{Model}_1 = R1 + R2 + R3 + R4 + R5 + R6 + R7 + R8$$

808 **Model_2_Clear**

809

810 $n(0)$ = percent persistence (organism level); $n(1)$ = density – levels mean (organism level); $n(2)$ = SD –
811 levels mean (well level); $n(3)$ = density – levels mean (well level) ; $n(4)$ = pinch mean (organism level) ;
812 $n(5)$ = model_1 (organism level) ; $n(6)$ = area mean (organism level)

$$\begin{aligned}
813 \quad R1 = & 3050.53971 + -15.56494 * n(0) + -0.83465 * n(1) + -4.70861 * n(2) + -1.83172 * n(3) + - \\
814 \quad & 1087.22384 * n(4) + -1798.96904 * n(5) + 0.00388693 * n(6) + 0.00701913 * n(0) * n(1) + 0.00621377 * \\
815 \quad & n(0) * n(2) + 0.012155 * n(0) * n(3) + 1.18447 * n(0) * n(4) + 3.5422 * n(0) * n(5) + 0.000836635 * n(0) * \\
816 \quad & n(6)
\end{aligned}$$

$$\begin{aligned}
817 \quad R2 = & 0.00167653 * n(1) * n(2) + 0.000382736 * n(1) * n(3) + 0.82585 * n(1) * n(4) + 0.48752 * n(1) * \\
818 \quad & n(5) + -0.0000204636 * n(1) * n(6) + 0.00409758 * n(2) * n(3) + 0.22639 * n(2) * n(4) + 0.50064 * n(2) * \\
819 \quad & n(5) + 0.00000930964 * n(2) * n(6) + -0.2123 * n(3) * n(4) + 1.34517 * n(3) * n(5) + -0.000049354 * n(3) \\
820 \quad & * n(6) + 467.08521 * n(4) * n(5) + 0.065277 * n(4) * n(6)
\end{aligned}$$

$$\begin{aligned}
821 \quad R3 = & 0.022834 * n(5) * n(6) + -0.032424 * n(0) ^ 2 + -0.00016082 * n(1) ^ 2 + 0.000283988 * n(2) ^ 2 + \\
822 \quad & 0.0000706305 * n(3) ^ 2 + 665.10179 * n(4) ^ 2 + 297.72877 * n(5) ^ 2 + -0.00000288682 * n(6) ^ 2 + \\
823 \quad & 0.000000576592 * n(0) * n(1) * n(2) + -0.00000550441 * n(0) * n(1) * n(3) + -0.00344384 * n(0) * n(1) * \\
824 \quad & n(4) + -0.000418887 * n(0) * n(1) * n(5) + -0.00000000266297 * n(0) * n(1) * n(6) + -0.00000537496 * \\
825 \quad & n(0) * n(2) * n(3)
\end{aligned}$$

$$\begin{aligned}
826 \quad R4 = & 0.00123966 * n(0) * n(2) * n(4) + -0.000539946 * n(0) * n(2) * n(5) + -0.000000269514 * n(0) * n(2) \\
827 \quad & * n(6) + 0.000685879 * n(0) * n(3) * n(4) + -0.00295768 * n(0) * n(3) * n(5) + -0.000000600777 * n(0) * \\
828 \quad & n(3) * n(6) + 0.45772 * n(0) * n(4) * n(5) + -0.0000773276 * n(0) * n(4) * n(6) + -0.0000149499 * n(0) * \\
829 \quad & n(5) * n(6) + -0.00000121635 * n(1) * n(2) * n(3) + 0.0000187735 * n(1) * n(2) * n(4) + -0.000393188 * \\
830 \quad & n(1) * n(2) * n(5) + -0.00000000836334 * n(1) * n(2) * n(6) + 0.000237552 * n(1) * n(3) * n(4)
\end{aligned}$$

$$\begin{aligned}
831 \quad R5 = & -0.000170248 * n(1) * n(3) * n(5) + 0.0000000424461 * n(1) * n(3) * n(6) + -0.13473 * n(1) * n(4) * \\
832 \quad & n(5) + -0.0000398496 * n(1) * n(4) * n(6) + -0.00000609553 * n(1) * n(5) * n(6) + -0.000155192 * n(2) *
\end{aligned}$$

833 $n(3) * n(4) + -0.000135105 * n(2) * n(3) * n(5) + -0.00000000770149 * n(2) * n(3) * n(6) + 0.12141 * n(2)$
 834 $* n(4) * n(5) + 0.00000677018 * n(2) * n(4) * n(6) + -0.0000221139 * n(2) * n(5) * n(6) + -0.17437 * n(3)$
 835 $* n(4) * n(5) + -0.0000342233 * n(3) * n(4) * n(6) + 0.00000269916 * n(3) * n(5) * n(6)$

836 $R6 = -0.014 * n(4) * n(5) * n(6) + -0.00000661836 * n(0) ^ 2 * n(1) + -0.00000267154 * n(0) ^ 2 * n(2) +$
 837 $0.0000291939 * n(0) ^ 2 * n(3) + 0.00558697 * n(0) ^ 2 * n(4) + 0.00128265 * n(0) ^ 2 * n(5) +$
 838 $0.00000138321 * n(0) ^ 2 * n(6) + 0.00000042153 * n(0) * n(1) ^ 2 + -0.000001289 * n(0) * n(2) ^ 2 + -$
 839 $0.00000234632 * n(0) * n(3) ^ 2 + 1.26238 * n(0) * n(4) ^ 2 + -0.17282 * n(0) * n(5) ^ 2 + -$
 840 $0.0000000408076 * n(0) * n(6) ^ 2 + -0.000000130828 * n(1) ^ 2 * n(2)$

841 $R7 = 0.000000125061 * n(1) ^ 2 * n(3) + -0.000289823 * n(1) ^ 2 * n(4) + -0.000023126 * n(1) ^ 2 * n(5)$
 842 $+ -0.0000001232 * n(1) * n(2) ^ 2 + -0.000000121779 * n(1) * n(3) ^ 2 + -0.23081 * n(1) * n(4) ^ 2 + -$
 843 $0.16611 * n(1) * n(5) ^ 2 + 0.000000158732 * n(2) ^ 2 * n(3) + -0.0000495972 * n(2) ^ 2 * n(4) +$
 844 $0.000141303 * n(2) ^ 2 * n(5) + 0.0000000097208 * n(2) ^ 2 * n(6) + -0.00000110647 * n(2) * n(3) ^ 2 +$
 845 $-0.10298 * n(2) * n(4) ^ 2 + 0.026119 * n(2) * n(5) ^ 2$

846 $R8 = 0.00000000227912 * n(2) * n(6) ^ 2 + 0.000183837 * n(3) ^ 2 * n(4) + -0.000396325 * n(3) ^ 2 *$
 847 $n(5) + 0.0000000245561 * n(3) ^ 2 * n(6) + -0.31387 * n(3) * n(4) ^ 2 + -0.033724 * n(3) * n(5) ^ 2 +$
 848 $0.000000000433223 * n(3) * n(6) ^ 2 + -126.01624 * n(4) ^ 2 * n(5) + -0.00723282 * n(4) ^ 2 * n(6) + -$
 849 $88.82786 * n(4) * n(5) ^ 2 + 0.00000545089 * n(4) * n(6) ^ 2 + -0.012727 * n(5) ^ 2 * n(6) + -$
 850 $0.000000923552 * n(5) * n(6) ^ 2 + 0.000027338 * n(0) ^ 3$

851 $R9 = 0.0000000615183 * n(1) ^ 3 + -0.00000021971 * n(2) ^ 3 + 0.000000176908 * n(3) ^ 3 + -$
 852 $60.56525 * n(4) ^ 3 + -13.42882 * n(5) ^ 3 + 0.000000000125105 * n(6) ^ 3 + 8.83587E-11 * n(0) * n(1)$
 853 $* n(2) * n(6) + 0.00000163142 * n(0) * n(1) * n(3) * n(4) + 0.000000287771 * n(0) * n(1) * n(3) * n(5) + -$
 854 $0.000188377 * n(0) * n(1) * n(4) * n(5) + -0.000000867302 * n(0) * n(2) * n(3) * n(4) +$
 855 $0.000000000132956 * n(0) * n(2) * n(3) * n(6) + 0.000514007 * n(0) * n(2) * n(4) * n(5) + -$
 856 $0.0000000938365 * n(0) * n(2) * n(4) * n(6)$

857 $R10 = -0.000256585 * n(0) * n(3) * n(4) * n(5) + 0.000000144641 * n(0) * n(3) * n(4) * n(6) +$
 858 $0.00000017782 * n(1) * n(2) * n(3) * n(5) + -0.000033291 * n(1) * n(2) * n(4) * n(5) + 0.00000000921168$
 859 $* n(1) * n(2) * n(5) * n(6) + -0.0000684562 * n(1) * n(3) * n(4) * n(5) + 0.0000000189874 * n(1) * n(3) *$
 860 $n(4) * n(6) + -0.00013601 * n(2) * n(3) * n(4) * n(5) + -0.00000000626452 * n(2) * n(3) * n(5) * n(6) +$
 861 $0.0000154375 * n(2) * n(4) * n(5) * n(6) + 0.0000000022209 * n(0) ^ 2 * n(1) ^ 2 + -0.00000000030416$
 862 $* n(0) ^ 2 * n(1) * n(6) + -0.00000000197509 * n(0) ^ 2 * n(2) ^ 2 + 0.00000301416 * n(0) ^ 2 * n(2) *$
 863 $n(4)$

864 $R11 = -0.00000000426287 * n(0) ^ 2 * n(3) ^ 2 + -0.00000500198 * n(0) ^ 2 * n(3) * n(4) + -$
 865 $0.00000142532 * n(0) ^ 2 * n(3) * n(5) + -0.000000000528475 * n(0) ^ 2 * n(3) * n(6) + 0.00075716 *$
 866 $n(0) ^ 2 * n(4) ^ 2 + 0.00120644 * n(0) ^ 2 * n(4) * n(5) + 0.000000207233 * n(0) ^ 2 * n(4) * n(6) + -$
 867 $0.000000000324208 * n(0) * n(1) ^ 2 * n(2) + -0.000000000244258 * n(0) * n(1) ^ 2 * n(3) +$
 868 $0.000000000461462 * n(0) * n(1) * n(2) ^ 2 + 0.00000000112886 * n(0) * n(1) * n(3) ^ 2 +$
 869 $0.000000635517 * n(0) * n(2) ^ 2 * n(4) + -0.000000000036482 * n(0) * n(2) ^ 2 * n(6) +$
 870 $0.000000001308 * n(0) * n(2) * n(3) ^ 2$

$$\begin{aligned}
& R12 = -0.000206579 * n(0) * n(2) * n(4) ^ 2 + -1.17651E-11 * n(0) * n(2) * n(6) ^ 2 + -0.000000833799 * \\
& n(0) * n(3) ^ 2 * n(4) + 0.000000636733 * n(0) * n(3) ^ 2 * n(5) + 0.000000000061738 * n(0) * n(3) ^ 2 * \\
& n(6) + 0.0000662669 * n(0) * n(3) * n(5) ^ 2 + 2.40122E-11 * n(0) * n(3) * n(6) ^ 2 + -0.0000818538 * \\
& n(0) * n(4) ^ 2 * n(6) + 0.043108 * n(0) * n(4) * n(5) ^ 2 + -0.00000000647759 * n(0) * n(4) * n(6) ^ 2 + \\
& 0.00000000165957 * n(0) * n(5) * n(6) ^ 2 + -0.0000000014381 * n(1) ^ 2 * n(2) ^ 2 + - \\
& 0.000000000318973 * n(1) ^ 2 * n(2) * n(3) + 0.0000000115171 * n(1) ^ 2 * n(2) * n(4)
\end{aligned}$$

$$\begin{aligned}
& R13 = 0.000000119935 * n(1) ^ 2 * n(3) * n(4) + -0.000000100809 * n(1) ^ 2 * n(3) * n(5) + \\
& 0.0000705524 * n(1) ^ 2 * n(4) * n(5) + 0.00000619885 * n(1) ^ 2 * n(5) ^ 2 + 0.000000000267632 * \\
& n(1) * n(2) ^ 2 * n(3) + -0.000000051141 * n(1) * n(2) ^ 2 * n(4) + 0.000000000524427 * n(1) * n(2) * \\
& n(3) ^ 2 + -0.000000268552 * n(1) * n(3) ^ 2 * n(4) + 0.000000121555 * n(1) * n(3) ^ 2 * n(5) + - \\
& 1.48346E-11 * n(1) * n(3) ^ 2 * n(6) + 0.000110143 * n(1) * n(3) * n(4) ^ 2 + 0.0000487937 * n(1) * n(3) \\
& * n(5) ^ 2 + 0.021921 * n(1) * n(4) * n(5) ^ 2 + 0.00000346283 * n(1) * n(5) ^ 2 * n(6)
\end{aligned}$$

$$\begin{aligned}
& R14 = -0.000000000177114 * n(2) ^ 2 * n(3) ^ 2 + 0.0000000210209 * n(2) ^ 2 * n(3) * n(4) + - \\
& 0.0000000818784 * n(2) ^ 2 * n(3) * n(5) + 0.0000376644 * n(2) ^ 2 * n(4) * n(5) + -9.31503E-13 * n(2) ^ 2 * \\
& n(6) ^ 2 + 0.000106985 * n(2) * n(3) * n(4) ^ 2 + 0.055031 * n(2) * n(4) ^ 2 * n(5) + -0.035459 * n(2) * \\
& n(4) * n(5) ^ 2 + 0.0000755324 * n(3) ^ 2 * n(4) * n(5) + -0.0000189566 * n(3) ^ 2 * n(5) ^ 2 + 0.040084 \\
& * n(3) * n(4) ^ 2 * n(5) + -0.00000000234695 * n(3) * n(4) * n(6) ^ 2 + 17.20136 * n(4) ^ 2 * n(5) ^ 2 + \\
& 0.004504 * n(4) * n(5) ^ 2 * n(6)
\end{aligned}$$

$$\begin{aligned}
& R15 = 0.000000561702 * n(4) * n(5) * n(6) ^ 2 + 0.0000000479781 * n(5) ^ 2 * n(6) ^ 2 + - \\
& 0.00000000944116 * n(0) ^ 3 * n(1) + 0.0000000115184 * n(0) ^ 3 * n(2) + -0.0000000158032 * n(0) ^ 3 * \\
& n(3) + 0.00000536878 * n(0) ^ 3 * n(4) + 0.00000362103 * n(0) ^ 3 * n(5) + 0.00000000106752 * n(0) \\
& ^ 3 * n(6) + -0.31887 * n(0) * n(4) ^ 3 + -0.00358755 * n(0) * n(5) ^ 3 + 0.000000000155012 * n(1) ^ 3 * \\
& n(2) + 0.000000025693 * n(1) ^ 3 * n(5) + 8.47252E-11 * n(1) * n(2) ^ 3 + 0.0000000269769 * n(2) ^ 3 * \\
& n(4)
\end{aligned}$$

$$\begin{aligned}
& R16 = -0.040793 * n(2) * n(4) ^ 3 + 0.013965 * n(2) * n(5) ^ 3 + 0.0000000679358 * n(3) ^ 3 * n(4) + \\
& 0.00494237 * n(4) ^ 3 * n(6) + 0.000439059 * n(5) ^ 3 * n(6) + 3.26886E-11 * n(5) * n(6) ^ 3 + \\
& 0.0000000400428 * n(0) ^ 4 + -1.89276E-11 * n(1) ^ 4 + -3.18337E-11 * n(3) ^ 4 + 25.12615 * n(4) ^ 4 \\
& + 2.44964 * n(5) ^ 4 + -7.13436E-15 * n(6) ^ 4 + 0 + 0
\end{aligned}$$

$$\begin{aligned}
& \text{Model_2_Clear} = R1 + R2 + R3 + R4 + R5 + R6 + R7 + R8 + R9 + R10 + R11 + R12 + R13 + R14 + \\
& R15 + R16
\end{aligned}$$

901

902 **Model_3_Clear**

903

904 n(0) = percent persistence (organism level); n(1) = form factor mean (organism level); n(2) = density –
 905 levels mean (well level) ; n(3) = model_1 (organism level) ; n(4) = model_2_clear (organism level)

$$\begin{aligned}
& R1 = 32.52402 + -0.54831 * n(0) + 55.81306 * n(1) + -0.029513 * n(2) + 13.34291 * n(3) + 13.05986 * \\
& n(4)
\end{aligned}$$

$$\begin{aligned}
& R2 = 0.16126 * n(0) * n(1) + 0.000562305 * n(0) * n(2) + 0.11982 * n(0) * n(3) + -0.08123 * n(0) * n(4) + \\
& -0.062883 * n(1) * n(2) + 5.31126 * n(1) * n(3)
\end{aligned}$$

910 $R3 = -4.81 * n(1) * n(4) + -0.021003 * n(2) * n(3) + -0.00540019 * n(2) * n(4) + -0.70453 * n(3) * n(4) + -$
 911 $0.00140765 * n(0) ^ 2 + 9.04074 * n(1) ^ 2$

912 $R4 = 0.00000723861 * n(2) ^ 2 + 0.11459 * n(3) ^ 2 + -1.78504 * n(4) ^ 2 + -0.0000819342 * n(0) * n(1)$
 913 $* n(2) + -0.021891 * n(0) * n(1) * n(3) + 0.013961 * n(0) * n(1) * n(4)$

914 $R5 = -0.0000529987 * n(0) * n(2) * n(3) + 0.0000474044 * n(0) * n(2) * n(4) + 0.000387712 * n(0) ^ 2 *$
 915 $n(1) + 0.000000947006 * n(0) ^ 2 * n(2) + 0.0000959058 * n(0) ^ 2 * n(3) + -0.000237815 * n(0) ^ 2 *$
 916 $n(4)$

917 $R6 = -0.04276 * n(0) * n(1) ^ 2 + -0.000000154351 * n(0) * n(2) ^ 2 + 0.00112266 * n(0) * n(4) ^ 2 + -$
 918 $2.45185 * n(1) ^ 2 * n(3) + 2.50057 * n(1) ^ 2 * n(4) + 0.0000161108 * n(1) * n(2) ^ 2$

919 $R7 = 0.40533 * n(1) * n(4) ^ 2 + 0.00000632871 * n(2) ^ 2 * n(3) + 0.00083054 * n(2) * n(4) ^ 2 + -$
 920 $0.45553 * n(3) ^ 2 * n(4) + 0.87222 * n(3) * n(4) ^ 2 + -0.0000031075 * n(0) ^ 3$

921 $R8 = -2.84358 * n(1) ^ 3 + 0.14201 * n(3) ^ 3 + -0.38692 * n(4) ^ 3 + 0 + 0 + 0$

922 $Model_3_Clear = R1 + R2 + R3 + R4 + R5 + R6 + R7 + R8$

923

924 **Model_2_Dark**

925

926 $n(0)$ = density – levels mean (organism level); $n(1)$ = SD – levels mean (organism level); $n(2)$ = percent
 927 persistence (well level); $n(3)$ = SD – levels mean (well level); $n(4)$ = pinch mean (organism level); $n(5)$ =
 928 $model_1$ (organism level)

929 $R1 = -361.12162 + 0.56347 * n(0) + 1.91376 * n(1) + -4.00323 * n(2) + -0.013169 * n(3) + -139.20978 *$
 930 $n(4) + 218.65312 * n(5) + -0.00153984 * n(0) * n(1) + 0.0052126 * n(0) * n(2) + -0.000454827 * n(0) *$
 931 $n(3) + -0.050456 * n(0) * n(4) + -0.18053 * n(0) * n(5) + -0.024777 * n(1) * n(2) + -0.00141908 * n(1) *$
 932 $n(3) + -0.12855 * n(1) * n(4) + -0.15031 * n(1) * n(5) + 0.011171 * n(2) * n(3) + 2.32431 * n(2) * n(4) + -$
 933 $2.09687 * n(2) * n(5) + 0.53271 * n(3) * n(4) + -0.027043 * n(3) * n(5)$

934 $R2 = 12.99119 * n(4) * n(5) + -0.000309284 * n(0) ^ 2 + -0.000849861 * n(1) ^ 2 + 0.043616 * n(2) ^ 2 +$
 935 $-0.000056373 * n(3) ^ 2 + 124.14887 * n(4) ^ 2 + -56.25437 * n(5) ^ 2 + 0.0000128757 * n(0) * n(1) *$
 936 $n(2) + 0.00000098784 * n(0) * n(1) * n(3) + 0.000182684 * n(0) * n(1) * n(4) + 0.00002946 * n(0) * n(1) *$
 937 $n(5) + -0.00000513663 * n(0) * n(2) * n(3) + -0.000177285 * n(0) * n(2) * n(4) + 0.0000739509 * n(0) *$
 938 $n(2) * n(5) + -0.000231917 * n(0) * n(3) * n(4) + 0.0000143359 * n(0) * n(3) * n(5) + 0.051313 * n(0) *$
 939 $n(4) * n(5) + 0.00000505626 * n(1) * n(2) * n(3) + -0.000114908 * n(1) * n(2) * n(4) + 0.0036413 * n(1) *$
 940 $n(2) * n(5) + -0.000463003 * n(1) * n(3) * n(4)$

941 $R3 = 0.000195403 * n(1) * n(3) * n(5) + 0.027341 * n(1) * n(4) * n(5) + -0.0057082 * n(2) * n(3) * n(4) + -$
 942 $0.00151504 * n(2) * n(3) * n(5) + -0.37303 * n(2) * n(4) * n(5) + -0.032101 * n(3) * n(4) * n(5) +$
 943 $0.000000363092 * n(0) ^ 2 * n(1) + -0.00000126177 * n(0) ^ 2 * n(2) + 0.000000335253 * n(0) ^ 2 * n(3)$
 944 $+ 0.00000930206 * n(0) ^ 2 * n(4) + 0.0000630895 * n(0) ^ 2 * n(5) + 0.000000625327 * n(0) * n(1) ^ 2$
 945 $+ -0.0000534651 * n(0) * n(2) ^ 2 + -0.0000000239318 * n(0) * n(3) ^ 2 + -0.00396581 * n(0) * n(4) ^ 2$
 946 $+ 0.023233 * n(0) * n(5) ^ 2 + 0.00000989143 * n(1) ^ 2 * n(2) + 0.00000105728 * n(1) ^ 2 * n(3) + -$
 947 $0.000160825 * n(1) ^ 2 * n(4) + 0.0000106839 * n(1) ^ 2 * n(5) + 0.0000984379 * n(1) * n(2) ^ 2$

948 $R4 = 0.000000294665 * n(1) * n(3) ^ 2 + 0.026272 * n(1) * n(4) ^ 2 + -0.021385 * n(1) * n(5) ^ 2 + -$
949 $0.00000220276 * n(2) ^ 2 * n(3) + 0.00809653 * n(2) ^ 2 * n(4) + 0.018287 * n(2) ^ 2 * n(5) + -$
950 $0.00000561739 * n(2) * n(3) ^ 2 + -1.65978 * n(2) * n(4) ^ 2 + 0.50979 * n(2) * n(5) ^ 2 + 0.000142765 * n(3) ^ 2 * n(4) + 0.0000247584 * n(3) ^ 2 * n(5) + -0.10679 * n(3) * n(4) ^ 2 + 0.030073 * n(3) * n(5) ^ 2$
951 $+ -54.71951 * n(4) ^ 2 * n(5) + 5.80519 * n(4) * n(5) ^ 2 + 0.000000067095 * n(0) ^ 3 + -$
952 $0.000000310388 * n(1) ^ 3 + -0.000236629 * n(2) ^ 3 + 0.000000169864 * n(3) ^ 3 + -6.52428 * n(4) ^ 3$
953 $+ 5.28688 * n(5) ^ 3$

955 $R5 = 0.000000128977 * n(0) * n(1) * n(3) * n(4) + -0.0000000405581 * n(0) * n(1) * n(3) * n(5) + -$
956 $0.0000552203 * n(0) * n(1) * n(4) * n(5) + 0.000000890618 * n(0) * n(2) * n(3) * n(4) + 0.000000325049$
957 $* n(0) * n(2) * n(3) * n(5) + 0.00000169698 * n(1) * n(2) * n(3) * n(4) + -0.000000758555 * n(1) * n(2) *$
958 $n(3) * n(5) + 0.00057653 * n(2) * n(3) * n(4) * n(5) + -6.57659E-11 * n(0) ^ 2 * n(1) ^ 2 + -$
959 $0.00000000245433 * n(0) ^ 2 * n(1) * n(2) + -0.00000000022752 * n(0) ^ 2 * n(1) * n(3) +$
960 $0.0000000214646 * n(0) ^ 2 * n(1) * n(4) + 0.0000000125412 * n(0) ^ 2 * n(2) ^ 2 +$
961 $0.000000000904972 * n(0) ^ 2 * n(2) * n(3) + 4.11355E-11 * n(0) ^ 2 * n(3) ^ 2 + 0.0000000265477 *$
962 $n(0) ^ 2 * n(3) * n(4) + -0.0000104834 * n(0) ^ 2 * n(4) * n(5) + -0.00000366468 * n(0) ^ 2 * n(5) ^ 2 + -$
963 $0.00000000218385 * n(0) * n(1) ^ 2 * n(2) + -0.000000000175384 * n(0) * n(1) ^ 2 * n(3) + -$
964 $0.00000000678748 * n(0) * n(1) ^ 2 * n(4)$

965 $R6 = -0.0000000209727 * n(0) * n(1) * n(2) ^ 2 + -0.000000000109807 * n(0) * n(1) * n(3) ^ 2 + -$
966 $0.0000800513 * n(0) * n(1) * n(4) ^ 2 + 0.0000145427 * n(0) * n(1) * n(5) ^ 2 + -0.00000000641016 *$
967 $n(0) * n(2) ^ 2 * n(3) + -0.00000476213 * n(0) * n(2) ^ 2 * n(4) + 0.00000000101544 * n(0) * n(2) * n(3) ^ 2$
968 $+ 0.000304876 * n(0) * n(2) * n(4) ^ 2 + -0.0000663645 * n(0) * n(2) * n(5) ^ 2 + -0.0000000404017 *$
969 $n(0) * n(3) ^ 2 * n(4) + 0.0000394658 * n(0) * n(3) * n(4) ^ 2 + -0.00000946448 * n(0) * n(3) * n(5) ^ 2 +$
970 $0.013504 * n(0) * n(4) ^ 2 * n(5) + -0.00662779 * n(0) * n(4) * n(5) ^ 2 + -0.000000035197 * n(1) ^ 2 *$
971 $n(2) ^ 2 + -0.0000000101636 * n(1) ^ 2 * n(2) * n(3) + 0.000000190077 * n(1) ^ 2 * n(3) * n(4) +$
972 $0.0000734302 * n(1) ^ 2 * n(4) ^ 2 + 0.0000483842 * n(1) ^ 2 * n(4) * n(5) + -0.0000000182885 * n(1) *$
973 $n(2) ^ 2 * n(3) + -0.0000227993 * n(1) * n(2) ^ 2 * n(5)$

974 $R7 = 0.00000000324656 * n(1) * n(2) * n(3) ^ 2 + -0.0000941191 * n(1) * n(2) * n(5) ^ 2 + -$
975 $0.0000000755622 * n(1) * n(3) ^ 2 * n(5) + 0.010924 * n(1) * n(4) * n(5) ^ 2 + 0.0000000126476 * n(2) ^ 2$
976 $* n(3) ^ 2 + 0.0000114672 * n(2) ^ 2 * n(3) * n(4) + 0.00286912 * n(2) ^ 2 * n(4) ^ 2 + -0.00348402 *$
977 $n(2) ^ 2 * n(4) * n(5) + -0.00275424 * n(2) ^ 2 * n(5) ^ 2 + 0.000000519982 * n(2) * n(3) ^ 2 * n(5) +$
978 $0.000450946 * n(2) * n(3) * n(4) ^ 2 + 0.31246 * n(2) * n(4) ^ 2 * n(5) + 3.02457 * n(4) ^ 2 * n(5) ^ 2 + -$
979 $2.00237E-11 * n(0) ^ 3 * n(1) + -0.000000000070125 * n(0) ^ 3 * n(3) + -0.00000000793741 * n(0) ^ 3 *$
980 $n(5) + -0.000000000158606 * n(0) * n(1) ^ 3 + 0.0000000785055 * n(0) * n(2) ^ 3 + -9.21427E-11 * n(0)$
981 $* n(3) ^ 3 + -0.011845 * n(0) * n(4) ^ 3 + 0.00000000297869 * n(1) ^ 3 * n(2)$

982 $R8 = -0.000000000243674 * n(1) ^ 3 * n(3) + -0.0000000759836 * n(1) ^ 3 * n(5) + -0.00000000015798$
983 $* n(1) * n(3) ^ 3 + 0.031905 * n(1) * n(4) ^ 3 + -0.00308156 * n(1) * n(5) ^ 3 + -0.0000000397407 * n(3)$
984 $^ 3 * n(4) + -0.0000000277537 * n(3) ^ 3 * n(5) + -0.0022742 * n(3) * n(5) ^ 3 + -0.72285 * n(4) * n(5) ^ 3$
985 $+ -3.17195E-12 * n(0) ^ 4 + 0.000000000456645 * n(1) ^ 4 + 0.000000336111 * n(2) ^ 4 + 7.93096E-$
986 $11 * n(3) ^ 4 + 6.09015 * n(4) ^ 4 + -0.31393 * n(5) ^ 4 + 0 + 0 + 0 + 0 + 0$

987 $Model_2_Dark = R1 + R2 + R3 + R4 + R5 + R6 + R7 + R8$

988

989 **Model_3_Dark**

990

991 n(0) = percent persistence (organism level); n(1) = x-y position stdev (organism level); n(2) = area
992 mean (organism level); n(3) = area stdev (organism level); n(4) = SD – levels stdev (organism level);
993 n(5) model_1 (organism level); n(6) model_2 (organism level);

994 $R1 = -4.61017 + 0.092707 * n(0) + 0.35653 * n(1) + 0.000750986 * n(2) + -0.00452111 * n(3) +$
995 $0.011807 * n(4) + 5.71269 * n(5) + -1.49563 * n(6) + -0.00976856 * n(0) * n(1) + -0.0000263884 * n(0) *$
996 $n(2) + 0.000135389 * n(0) * n(3) + 0.000208516 * n(0) * n(4) + -0.08961 * n(0) * n(5) + 0.013908 * n(0)$
997 $* n(6)$

998 $R2 = 0.000111107 * n(1) * n(2) + -0.000521866 * n(1) * n(3) + -0.02206 * n(1) * n(4) + -0.39836 * n(1) *$
999 $n(5) + -0.32854 * n(1) * n(6) + -0.0000000992238 * n(2) * n(3) + 0.0000185838 * n(2) * n(4) + -$
1000 $0.000983153 * n(2) * n(5) + 0.000152417 * n(2) * n(6) + 0.0000626892 * n(3) * n(4) + 0.000877242 *$
1001 $n(3) * n(5) + 0.00418134 * n(3) * n(6) + 0.00787532 * n(4) * n(5) + 0.045654 * n(4) * n(6)$

1002 $R3 = 0.55274 * n(5) * n(6) + -0.00027944 * n(0) ^ 2 + -0.013183 * n(1) ^ 2 + 0.0000000794713 * n(2) ^$
1003 $2 + 0.00000436954 * n(3) ^ 2 + -0.000737969 * n(4) ^ 2 + -1.60087 * n(5) ^ 2 + 1.28554 * n(6) ^ 2 +$
1004 $0.00000121589 * n(0) * n(1) * n(2) + 0.000000680117 * n(0) * n(1) * n(3) + 0.000063997 * n(0) * n(1) *$
1005 $n(4) + 0.00737386 * n(0) * n(1) * n(5) + 0.00629009 * n(0) * n(1) * n(6) + -0.0000000203623 * n(0) *$
1006 $n(2) * n(3)$

1007 $R4 = 0.000000283108 * n(0) * n(2) * n(4) + 0.0000214193 * n(0) * n(2) * n(5) + -0.00000950404 * n(0) *$
1008 $n(2) * n(6) + 0.000000257292 * n(0) * n(3) * n(4) + -0.0000845602 * n(0) * n(3) * n(5) + -0.0000444008$
1009 $* n(0) * n(3) * n(6) + 0.00015789 * n(0) * n(4) * n(5) + -0.000189701 * n(0) * n(4) * n(6) +$
1010 $0.0000000668764 * n(1) * n(2) * n(3) + -0.00000226437 * n(1) * n(2) * n(4) + -0.0000495035 * n(1) *$
1011 $n(2) * n(5) + -0.0000570377 * n(1) * n(2) * n(6) + -0.0000110973 * n(1) * n(3) * n(4) + -0.0000984269 *$
1012 $n(1) * n(3) * n(5)$

1013 $R5 = -0.000547909 * n(1) * n(3) * n(6) + 0.000826802 * n(1) * n(4) * n(5) + -0.00174602 * n(1) * n(4) *$
1014 $n(6) + -0.034571 * n(1) * n(5) * n(6) + -0.0000000183872 * n(2) * n(3) * n(4) + 0.00000080816 * n(2) *$
1015 $n(3) * n(5) + 0.0000000300624 * n(2) * n(3) * n(6) + -0.0000272219 * n(2) * n(4) * n(5) + -0.0000091387$
1016 $* n(2) * n(4) * n(6) + -0.000119087 * n(2) * n(5) * n(6) + 0.0000690982 * n(3) * n(4) * n(5) +$
1017 $0.0000172096 * n(3) * n(4) * n(6) + -0.000273843 * n(3) * n(5) * n(6) + 0.00861831 * n(4) * n(5) * n(6)$

1018 $R6 = 0.0000303932 * n(0) ^ 2 * n(1) + 0.000000156693 * n(0) ^ 2 * n(2) + -0.000000170271 * n(0) ^ 2 *$
1019 $n(3) + -0.0000168954 * n(0) ^ 2 * n(4) + 0.000243014 * n(0) ^ 2 * n(5) + -0.0000186158 * n(0) ^ 2 * n(6)$
1020 $+ -0.000473015 * n(0) * n(1) ^ 2 + -0.000000000917335 * n(0) * n(2) ^ 2 + 0.0000000098126 * n(0) *$
1021 $n(3) ^ 2 + 0.00000251944 * n(0) * n(4) ^ 2 + 0.017146 * n(0) * n(5) ^ 2 + -0.000841143 * n(0) * n(6) ^ 2$
1022 $+ 0.0000110572 * n(1) ^ 2 * n(2) + 0.0000145286 * n(1) ^ 2 * n(3)$

1023 $R7 = 0.00205469 * n(1) ^ 2 * n(4) + 0.040184 * n(1) ^ 2 * n(5) + 0.060707 * n(1) ^ 2 * n(6) + -$
1024 $0.0000000343855 * n(1) * n(2) ^ 2 + 0.000000215682 * n(1) * n(3) ^ 2 + 0.000447475 * n(1) * n(4) ^ 2 +$
1025 $0.241 * n(1) * n(5) ^ 2 + 0.28481 * n(1) * n(6) ^ 2 + 0.000000000152796 * n(2) ^ 2 * n(3) + -$
1026 $0.000000000242684 * n(2) ^ 2 * n(4) + 0.000000000363359 * n(2) ^ 2 * n(5) + 0.00000012185 * n(2) ^ 2$
1027 $* n(6) + -0.000000000959079 * n(2) * n(3) ^ 2 + 0.00000018851 * n(2) * n(4) ^ 2$

1028 $R8 = 0.000173728 * n(2) * n(5) ^ 2 + -0.000284603 * n(2) * n(6) ^ 2 + 0.0000000102328 * n(3) ^ 2 * n(4) + -0.0000022087 * n(3) ^ 2 * n(5) + -0.0000000934567 * n(3) ^ 2 * n(6) + -0.00000105153 * n(3) * n(4) ^ 2 + -0.0000934181 * n(3) * n(5) ^ 2 + -0.00295776 * n(3) * n(6) ^ 2 + 0.000423315 * n(4) ^ 2 * n(5) + -0.0000799979 * n(4) ^ 2 * n(6) + -0.00450556 * n(4) * n(5) ^ 2 + -0.02169 * n(4) * n(6) ^ 2 + 0.26604 * n(5) * n(6) ^ 2 + -0.00000126558 * n(0) ^ 3$

1033 $R9 = -0.0039262 * n(1) ^ 3 + -4.15924E-12 * n(2) ^ 3 + -5.47209E-11 * n(3) ^ 3 + -0.0000191162 * n(4) ^ 3 + 0.059443 * n(5) ^ 3 + -0.49754 * n(6) ^ 3 + -0.000000000383815 * n(0) * n(1) * n(2) * n(3) + -0.000000750809 * n(0) * n(1) * n(2) * n(5) + -0.00000073033 * n(0) * n(1) * n(2) * n(6) + 0.0000000066314 * n(0) * n(1) * n(3) * n(4) + 0.00000157802 * n(0) * n(1) * n(3) * n(5) + 0.00000032997 * n(0) * n(1) * n(3) * n(6) + 0.0000444528 * n(0) * n(1) * n(4) * n(5) + 0.0000138956 * n(0) * n(1) * n(4) * n(6)$

1039 $R10 = 7.76253E-11 * n(0) * n(2) * n(3) * n(4) + 0.00000000959345 * n(0) * n(2) * n(3) * n(5) + 0.00000000542978 * n(0) * n(2) * n(3) * n(6) + -0.000000138988 * n(0) * n(2) * n(4) * n(5) + -0.000000255355 * n(0) * n(3) * n(4) * n(5) + 0.000000000366051 * n(1) * n(2) * n(3) * n(4) + -0.0000000198672 * n(1) * n(2) * n(3) * n(5) + 0.0000000271726 * n(1) * n(2) * n(3) * n(6) + 0.000000965152 * n(1) * n(2) * n(4) * n(5) + 0.00000090072 * n(1) * n(2) * n(4) * n(6) + 0.00000812757 * n(1) * n(3) * n(4) * n(5) + 0.00000797685 * n(1) * n(3) * n(4) * n(6) + 0.000103226 * n(1) * n(3) * n(5) * n(6) + -0.0000207396 * n(3) * n(4) * n(5) * n(6)$

1046 $R11 = -0.00000195856 * n(0) ^ 2 * n(1) ^ 2 + 0.0000000269254 * n(0) ^ 2 * n(1) * n(3) + -0.0000508801 * n(0) ^ 2 * n(1) * n(5) + 2.49496E-11 * n(0) ^ 2 * n(2) * n(3) + -0.0000000742936 * n(0) ^ 2 * n(2) * n(5) + 0.0000000306992 * n(0) ^ 2 * n(2) * n(6) + -0.000000000135004 * n(0) ^ 2 * n(3) ^ 2 + -0.00000000292662 * n(0) ^ 2 * n(3) * n(4) + 0.000000278337 * n(0) ^ 2 * n(3) * n(5) + 0.00000997994 * n(0) ^ 2 * n(4) * n(5) + -0.0000639369 * n(0) ^ 2 * n(6) ^ 2 + 0.0000000558002 * n(0) * n(1) ^ 2 * n(2) + -0.000000143373 * n(0) * n(1) ^ 2 * n(3) + -0.00000414178 * n(0) * n(1) ^ 2 * n(4)$

1052 $R12 = -0.000000000741061 * n(0) * n(1) * n(3) ^ 2 + -0.00000126359 * n(0) * n(1) * n(4) ^ 2 + -0.00203358 * n(0) * n(1) * n(6) ^ 2 + -2.37659E-13 * n(0) * n(2) ^ 2 * n(3) + 0.00000000033799 * n(0) * n(2) ^ 2 * n(6) + 1.08851E-12 * n(0) * n(2) * n(3) ^ 2 + -0.00000000142941 * n(0) * n(2) * n(4) ^ 2 + -0.00000293071 * n(0) * n(2) * n(5) ^ 2 + 0.00000237668 * n(0) * n(2) * n(6) ^ 2 + -8.93754E-11 * n(0) * n(3) ^ 2 * n(4) + 0.00000000419135 * n(0) * n(3) * n(4) ^ 2 + 0.00000995675 * n(0) * n(3) * n(6) ^ 2 + -0.000271624 * n(0) * n(4) * n(5) ^ 2 + -0.0000000015755 * n(1) ^ 2 * n(2) * n(3)$

1058 $R13 = -0.0000076574 * n(1) ^ 2 * n(2) * n(5) + -0.00000993414 * n(1) ^ 2 * n(2) * n(6) + -0.00000000914334 * n(1) ^ 2 * n(3) ^ 2 + 0.00000238695 * n(1) ^ 2 * n(3) * n(5) + -0.000688278 * n(1) ^ 2 * n(4) * n(5) + -0.000619047 * n(1) ^ 2 * n(4) * n(6) + -0.018618 * n(1) ^ 2 * n(6) ^ 2 + 0.0000000176265 * n(1) * n(2) ^ 2 * n(5) + 0.0000000156328 * n(1) * n(2) ^ 2 * n(6) + 0.000019277 * n(1) * n(2) * n(6) ^ 2 + -0.00000000110944 * n(1) * n(3) ^ 2 * n(4) + -0.0000000105332 * n(1) * n(3) ^ 2 * n(5) + -0.0000000252387 * n(1) * n(3) ^ 2 * n(6) + -0.0000000702263 * n(1) * n(3) * n(4) ^ 2$

1064 $R14 = 0.00012233 * n(1) * n(3) * n(6) ^ 2 + -0.000128546 * n(1) * n(4) ^ 2 * n(5) + -0.000106207 * n(1) * n(4) ^ 2 * n(6) + 0.0030741 * n(1) * n(4) * n(6) ^ 2 + -0.087995 * n(1) * n(5) * n(6) ^ 2 + 7.37175E-13 * n(2) ^ 2 * n(3) * n(4) + -9.59323E-11 * n(2) ^ 2 * n(3) * n(5) + -6.02571E-11 * n(2) ^ 2 * n(3) * n(6) + 2.50502E-12 * n(2) * n(3) ^ 2 * n(4) + 0.00000000442336 * n(2) * n(3) ^ 2 * n(5) + 9.93414E-11 * n(2) *$

1068 $n(3)^2 * n(6) + -6.40403E-11 * n(2) * n(3) * n(4)^2 + -0.000000292517 * n(2) * n(3) * n(5)^2 +$
1069 $0.00000955825 * n(2) * n(4) * n(5)^2$

1070 $R15 = 0.000000000350581 * n(3)^2 * n(4)^2 + -0.0000000168097 * n(3)^2 * n(4) * n(5) + -$
1071 $0.0000000161471 * n(3)^2 * n(4) * n(6) + -0.0000000692311 * n(3)^2 * n(5) * n(6) + -0.000020757 * n(3) * n(4) * n(5)^2 + 0.000617916 * n(3) * n(5) * n(6)^2 + 0.00021377 * n(4)^2 * n(5) * n(6) +$
1072 $0.000000339072 * n(0)^3 * n(1) + -0.00000000207837 * n(0)^3 * n(3) + 0.000019645 * n(0) * n(1)^3$
1073 $+ 4.45966E-14 * n(0) * n(2)^3 + 9.04952E-13 * n(0) * n(3)^3 + 0.0000000763313 * n(0) * n(4)^3 +$
1074 $0.00283387 * n(0) * n(6)^3$

1076 $R16 = 0.000000219559 * n(1)^3 * n(2) + 0.000000953974 * n(1)^3 * n(3) + -0.0000133042 * n(1)^3$
1077 $* n(4) + 0.000882434 * n(1)^3 * n(6) + -0.067623 * n(1) * n(5)^3 + 2.58842E-15 * n(2)^3 * n(3) + -$
1078 $9.82343E-12 * n(2)^3 * n(6) + 0.0000000054835 * n(3) * n(4)^3 + 0.000463001 * n(3) * n(5)^3 +$
1079 $0.000345934 * n(3) * n(6)^3 + 0.00000320697 * n(4)^3 * n(5) + 0.00000317484 * n(4)^3 * n(6) + -$
1080 $0.2124 * n(5) * n(6)^3 + -7.87648E-17 * n(3)^4$

1081 $R17 = 0.12069 * n(6)^4$

1082 $Model_3_Dark = R1 + R2 + R3 + R4 + R5 + R6 + R7 + R8 + R9 + R10 + R11 + R12 + R13 + R14 +$
1083 $R15 + R16 + R17$

1084
1085 **MySQL Database**

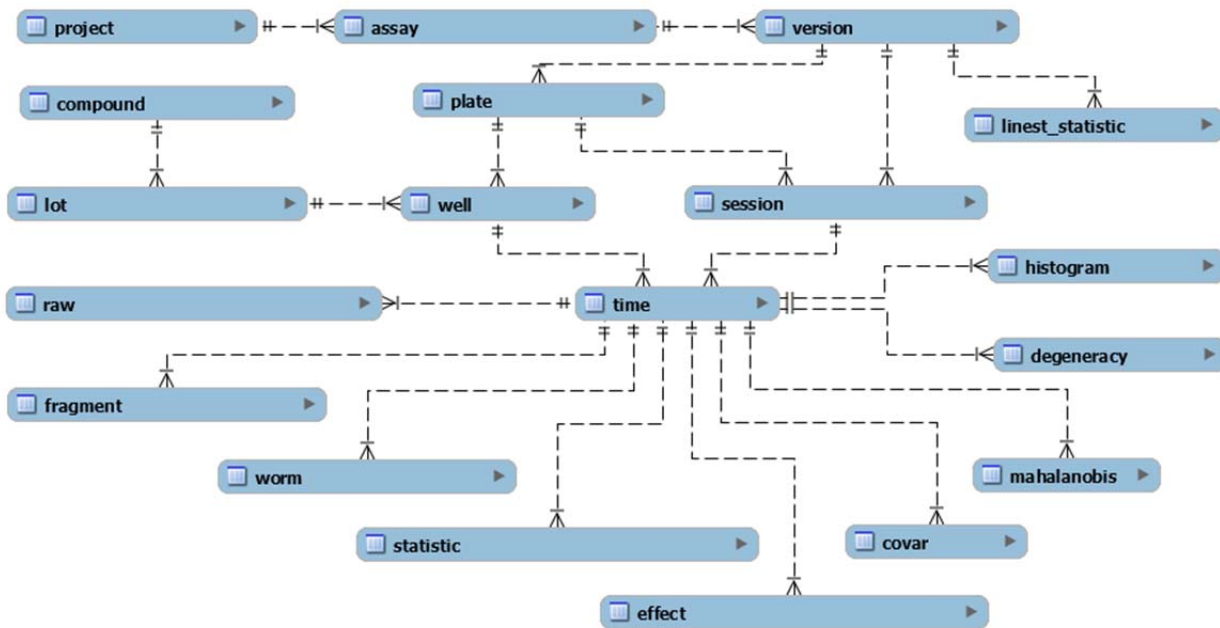
1086
1087 The experiment is defined in the database (**Figure 6**) by updating the “project”, “assay”,
1088 “version”, “plate”, “well”, “compound”, “lot”, and “session” tables. In the database, “version” is the
1089 version of the assay, “lot” is the version of the compound, and “session” stores the location of data files
1090 (data CSV, image acquisition XDCE), the date of the start of the iteration, and the status of the data
1091 processing. Next, the timestamp of every image is parsed and loaded into the “time” table. Then the file
1092 from data pre-processing is imported into the “raw” table and linked to the “time” table. The “time” table
1093 becomes the route to travel to different points in time within the same well whereas “session” is useful
1094 in separating the campaign into experimental iterations. The “time” table also stores flags indicating a
1095 well should not be considered for analysis. From the “raw” table, the data is processed and loaded into
1096 “frag”, “worm”, “result”, and “effect”.

1097 Data in the “raw” table were reorganized into “fragments”. Organisms in each time frame were
1098 linked to organisms in subsequent time frames using the method described in “Object Classification”
1099 steps 1 through 5. There is a chance that a link cannot be found or a link will be found a later time point.
1100 These gaps in the linking operation produce fragments of varying size. If the fragments are too small (<
1101 4 time points) the fragments are not used for analysis. Four or more time points per fragment ensures 3
1102 or more data points to estimate rate which is the mean amount of change per time frame.

1103 Long enough fragments in the “fragment” table were reorganized into “worms”. The “static”
1104 mean and standard deviation of each feature for all worm time points were calculated. The “rate” mean
1105 and standard deviation of each feature’s absolute change between time points were calculated. The
1106 “frequency” of each feature is determined by measuring the number of directional changes per time.
1107 Changes in value that are below the system noise were carried over if the change continues in the
1108 same direction. (**Table 2**).

1109
1110
1111
1112
1113
1114
1115
1116
1117
1118

The worms in the “worm” table are analyzed at the well level to provide results to the “results” table. The mean and standard deviation for “static”, “rate”, and frequency modes were calculated. Results in the “statistic” table are used to calculate effect sizes and Mahalanobis Distance in the “effects” table and “Mahalanobis” table. The Glass effect size is used to calculate effect sizes. The Mahalanobis Distance is calculated for the “static”, “rate” and “frequency” categories separately, the combination of “static” and “rate” categories, and the full combination of “static”, “rate”, and “frequency” categories. Degeneracy data is located in the “degeneracy” table. Degeneracy is the number of dark worms divided by the total worms per well.



1119
1120
1121
1122
1123
1124
1125
1126
1127
1128
1129
1130
1131
1132
1133
1134
1135
1136

Figure 6 MySQL database. A model of the database is shown with tables represented by blue boxes. Lines connecting boxes describe the relationship of the tables to each other.

1137
1138
1139
1140
1141
1142
1143
1144
1145

List of Features	Cutoff for "Clear"	Cutoff for "Opaque"
area	52.75	152
weighted_position_x	1.6	2.2
weighted_position_y	1.2	2.2
median_diameter	1.456	2.11
length	1.686	3.058
form_factor	0.0125	0.0155
perimeter	3.4485	5.569
straight_chord	1.659	2.8585
curved_chord	2.8105	4.372
custom_bend	0.0205	0.024
custom_pinch	0.025	0.0315
custom_wave	0.0225	0.0225
mass	7475.5	26395.5
weighted_moment_of_inertia	1.654	3.49
density_levels	4.445	2.3275
standard_deviation_of_density_levels	3.4245	1.8145
angle	2.059	3.232

1146
1147

1148 **Table 2 A measure of system noise per feature.** The table shows values for system noise per
 1149 feature. The system noise values are used to detect changes in motion that can be used to calculate
 1150 frequency.

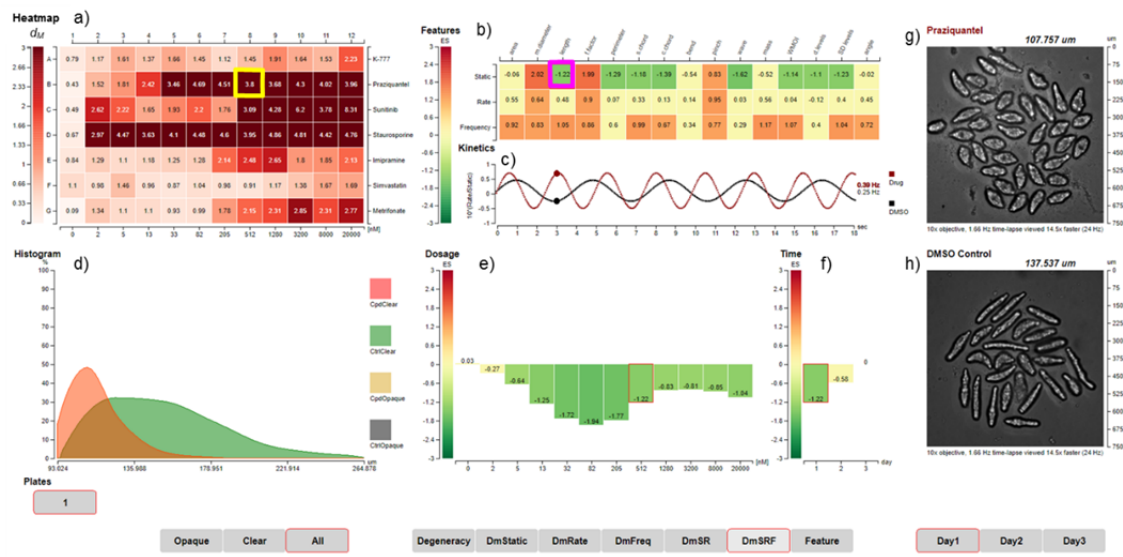
1151
 1152 **Graphical User Interface (GUI) of SchistoView**

1153
 1154 The GUI of SchistoView (**Figure 7**) allows hierarchical navigation of the experimental results. A
 1155 Mahalanobis Distance or percent degeneracy heatmap of the assay plate provides a high-level
 1156 summary. Selecting on a well in the heatmap updates the effect size heatmap which provides insight
 1157 into which features contribute to the well result. An effect size for a given feature may then be selected
 1158 to update the histogram of the well, the effect size plot over time, and the effect size dose response
 1159 for that feature. Frequency is visualized with an estimate of the waveform and displays the wavelength
 1160 and amplitude versus negative control DMSO. An image of the well at the indicated time point is
 1161 displayed.

1162 The user can toggle the campaigns, iterations within the campaign, data grouping, type of
 1163 Mahalanobis Distance (or percent degeneracy), effect category, and feature.

1164 SchistoView was created using Excel VBA forms and a MySQL connector to query the
 1165 database in real-time.

1166



1167

1168 **Figure 7.** Screenshot of the SchistoView graphical user interface. Selected data are shown to illustrate
 1169 the hierarchical approach to visualization. **(a)** Heat map of Mahalanobis distances (d_M) for seven test
 1170 drugs arrayed over an 11-point 2.5-fold dilution series from 2 nM in column 2 to 20 μM in column 12.
 1171 Drugs, from top to bottom, are, K1777, PZQ, sunitinib, staurosporine, imipramine, simvastatin and
 1172 metrifonate. DMSO controls are arrayed in column 1 and are shown as the average d_M (0.77) for all
 1173 DMSO controls. A d_M of 1.61 is significantly different (3 SD) from control. Clicking on coordinate B8
 1174 (identified by the yellow square: 512 nM PZQ) populates panels **(b)** and **(g)** (see below). **(b)** Heat map
 1175 showing the effect sizes (ES) for static, rate and frequency, after exposure to 512 nM PZQ for 2 h, *i.e.*,
 1176 the selected well from **(a)**. Three sets of 15 features are arrayed in rows and columns, respectively.
 1177 Clicking on the intersection of the length feature and static mode (magenta box) in **(b)** populates panels

1178 (c) through (f) and the underlying data. (c) Calculated waveforms defined by the range of length
1179 (amplitude) and frequency of length contraction (frequency). DMSO control worms are slower moving
1180 (lower frequency) than those treated with 512 nM PZQ (red line). (d) Histogram displaying the
1181 distribution of static length for DMSO control worms (green) and PZQ-treated worms (orange). (e) Bar
1182 graph depicting the ES for static length after PZQ treatment across 11 concentrations (second row in
1183 (a)). (f) Bar graph depicting the ES for static length in the 512 nM PZQ treatment across the three days
1184 of measurement. (g) First image from time-lapsed movie of the well highlighted in (a); in the live
1185 SchistoView, the 30-frame movie is looped. (h) as for (g) except for the DMSO control.